MOLECULAR IDENTIFICATION OF *LET-56* AND CHARACTERIZATION OF ITS REGULATORY ELEMENTS IN *CAENORHABDITIS ELEGANS*

by

Danyela Petra Lee

B.Sc., Simon Fraser University, 2007

THESIS SUBMITTED IN PARTIAL FULFILLMENT OF
THE REQUIREMENTS FOR THE DEGREE OF

MASTER OF SCIENCE

In the
Department of Molecular Biology and Biochemistry

© Danyela Petra Lee 2009

SIMON FRASER UNIVERSITY

Summer 2009

All rights reserved. This work may not be
reproduced in whole or in part, by photocopy
or other means, without permission of the author.

APPROVAL

Name: **Danyela Petra Lee**

Degree: **Master of Science**

Title of Thesis: **Molecular identification of *let-56* and characterization of its regulatory elements in *Caenorhabditis elegans***

Examining Committee:

Chair: **Dr. Peter C. Ruben**
Professor and Director, School of Kinesiology

_____

Dr. David L. Baillie
Senior Supervisor
Professor, Department of Molecular Biology and Biochemistry

_____

Dr. Nicholas Harden
Supervisor
Associate Professor, Department of Molecular Biology and Biochemistry

_____

Dr. Jack N. Chen
Supervisor
Associate Professor, Department of Molecular Biology and Biochemistry

_____

Dr. Frederic Pio
Internal Examiner
Associate Professor, Department of Molecular Biology and Biochemistry

Date Defended/Approved: May-19-2009

SFU SIMON FRASER UNIVERSITY
LIBRARY

Declaration of
Partial Copyright Licence

The author, whose copyright is declared on the title page of this work, has granted to Simon Fraser University the right to lend this thesis, project or extended essay to users of the Simon Fraser University Library, and to make partial or single copies only for such users or in response to a request from the library of any other university, or other educational institution, on its own behalf or for one of its users.

The author has further granted permission to Simon Fraser University to keep or make a digital copy for use in its circulating collection (currently available to the public at the "Institutional Repository" link of the SFU Library website <www.lib.sfu.ca> at: <http://ir.lib.sfu.ca/handle/1892/112>) and, without changing the content, to translate the thesis/project or extended essays, if technically possible, to any medium or format for the purpose of preservation of the digital work.

The author has further agreed that permission for multiple copying of this work for scholarly purposes may be granted by either the author or the Dean of Graduate Studies.

It is understood that copying or publication of this work for financial gain shall not be allowed without the author's written permission.

Permission for public performance, or limited permission for private scholarly use, of any multimedia materials forming part of this work, may have been granted by the author. This information may be found on the separately catalogued multimedia material and in the signed Partial Copyright Licence.

While licensing SFU to permit the above uses, the author retains copyright in the thesis, project or extended essays, including the right to change the work for subsequent purposes, including editing and publishing the work in whole or in part, and licensing other parties, as the author may desire.

The original Partial Copyright Licence attesting to these terms, and signed by this author, may be found in the original bound copy of this work, retained in the Simon Fraser University Archive.

Simon Fraser University Library
Burnaby, BC, Canada

ABSTRACT

let-56 was generated by EMS mutagenesis in a screen for essential genes in the *unc-22(IV)* region of *C. elegans.* The *let-56* locus is the largest developmentally required mutagenic target in the area. By sequencing seven of twelve alleles, I have determined the molecular identity of *let-56* to be *ZK829.4*, encoding glutamate dehydrogenase. GDH catalyzes the reversible formation of α-ketoglutarate and ammonia from glutamate, and mutations in GDH are associated with hyperinsulinism/hyperammonemia syndrome in humans. To gain better understanding of GDH activity, I have investigated mechanisms of its regulation. By analyzing *let-56*'s 5' promoter region, I have identified a 31bp window containing a transcription factor binding site. Using chimeric GFP reporter constructs, I have also demonstrated the importance of *let-56*'s 3' UTR in downregulating gene expression. In addition, by mimicking a mutation found in individuals with HI/HA, I have shown that *C. elegans* GDH also plays a role in insulin regulation.

ACKNOWLEDGEMENTS

I would like to thank my senior supervisor, Dr. David L. Baillie, for his patience, support, and encouragement, and for the opportunity to work in his laboratory. I would also like to thank the members of my supervisory committee, Drs. Nicholas Harden and Jack Chen, for their help and direction towards the completion of this thesis. In the Baillie lab, I would like to thank all members past and present, especially Carrie Simms, Drs. Bob Johnsen and Allan Mah for their advice, encouragement, and willingness to answer questions, and Domena Tu for the creation of all the transgenic strains used in the pursuit of this thesis. I would also like to thank ShuYi Chua, Rylan Fernandes, David Lee, Maha Al-Riyami, Dr. Martin Jones, and Nihar Bhattacharrya. I appreciate help provided by members of the Chen lab, especially Jeff Chu for his assistance with various methodologies and for sharing his bioinformatics expertise. I would also like to thank Marco Gallo of the Riddle lab for his advice and guidance in assaying increased insulin production, and Dr. Yuji Kohara for access to his EST database.

Most of all, I am grateful to my friends and family for their unwavering support during the pursuit of my degree and the completion of this thesis.

I would also like to acknowledge the funding of National Sciences and Engineering Research Council of Canada towards the completion of this research.

TABLE OF CONTENTS

Approval ..... **ii**

Abstract ..... **iii**

Acknowledgements ..... **iv**

Table of Contents ..... **v**

List of Figures ..... **viii**

List of Tables ..... **ix**

General Introduction **1**

Chapter 1: Determination of the molecular identity and the lethal arrest stage of *let-56* **7**

1.1 Introduction 7
1.1.1 The *unc-22(IV)* region and *let-56* 7
1.1.2 The lethal arrest stage of *let-56(s173)* 11
1.2 Materials and Methods 11
1.2.1 Nematode strains and culture conditions 11
1.2.2 Isolation of homozygous *let-56* individuals 11
1.2.3 Isolation of *C. elegans* genomic DNA 12
1.2.4 *ZK829.4* PCR amplification and sequencing 12
1.2.5 Sequence analysis 12
1.2.6 Microinjection 13
1.2.7 Fosmid PCR check 14
1.2.8 Rescue of *let-56* with fosmid *WRM069dG08* 14
1.2.9 Determination of *let-56(s173)* lethal arrest stage 15
1.2.10 Microscopy 15
1.3 Results 15
1.3.1 Sequencing results 15
1.3.2. Rescue of *let-56(s168)* with the fosmid *WRM069dG08* 16
1.3.3. The lethal arrest stage of *let-56(s173)* 17
1.4 Discussion 17

Chapter 2: Identification of a 5' *cis*-acting regulatory motif in the promotor region of *ZK829.4* **23**

2.1 Introduction 23
2.2 Materials and Methods 24
2.2.1 Construction of *let-56*$_{promoter}$::GFP transgenes 24
2.2.2 Microinjection 25
2.2.3 Microscopy 25

2.2.4 Comparison of the *ZK829.4* promoter to its *C. briggsae* orthologous region 26
2.2.5 *Cis*-regulatory element prediction 26
2.3 Results 26
2.3.1 Sequential *let-56*$_{promoter}$::GFP deletion constructs 26
2.3.2 Predicted *cis*-regulatory elements between -445bp and -414bp 30
2.4 Discussion 32

Chapter 3: Determination of the importance of the 3' UTR in regulation of *let-56* expression 38

3.1 Introduction 38
3.2 Materials and Methods 42
3.2.1 Total RNA extraction 42
3.2.2 Generation of cDNA samples 43
3.2.3 Quantitative RT-PCR 43
3.2.4 Generation of *ZK829.4*$_{promoter}$::GFP::3' UTR chimeric constructs 45
3.2.5 Generating competent DH5α cells 47
3.2.6 DH5α transformation 47
3.2.7 Microinjection 48
3.2.8 Transgene integration into the genome 48
3.2.9 Microscopy 48
3.3 Results 49
3.3.1 Quantitative RT-PCR 49
3.3.2 Chimeric GFP reporter constructs 51
3.4 Discussion 54

Chapter 4: The importance of the GTP-binding site in regulating GDH activity in C. elegans 58

4.1 Introduction 58
4.2 Materials and Methods 60
4.2.1 Construction of the GDH transgene with a GTP-binding site mutantion 60
4.2.2 Microinjection 62
4.2.3 Microscopy 62
4.3 Results 63
4.4 Discussion 63

General Discussion 66

Appendices 71

Appendix A. *let-56* strains used for sequence analysis. 71
Appendix B. ZK829.4 wildtype sequence and primers used for sequencing of *let-56* alleles 72
Appendix C. Forward primers used for *let-56* promoter amplification for *let-56*$_{promoter}$::GFP transgene constructs 74
Appendix D. *ZK829.4*$_{promoter}$::GFP strains 75
Appendix E. *C. elegans ZK829.4* and *C. briggsae* ortholog promoter sequences 76
Appendix F. *ZK829.*4$_{promoter}$::GFP expression analysis 77
Appendix G. ZK829.4$_{promoter}$::GFP::3' UTR strains 83

Appendix H. qRT-PCR results and sample calculation 84
Reference List.....85

LIST OF FIGURES

Figure 1. Isolating *let-56* candidate genes. 10

Figure 2. Extent of gonadal development in *let-56(s173)* homozygotes 19

Figure 3. GDH conservation and location of identified AA mutations in let-56 alleles 21

Figure 4. GFP expression levels of the different *ZK829.4*$_{promoter}$::GFP constructs 29

Figure 5. Sequence between -452bp and -391bp entered into TESS 31

Figure 6. Differences in GFP expression levels between segregant strains with the same promoter::GFP fusion 34

Figure 7. Predicted miRNA binding sites in the *let-56* 3' UTR 39

Figure 8. ZK829.4 3' UTR chimeric constructs 41

Figure 9. Location of primers used to detect the two ZK829.4 3' UTR transcripts by qRT-PCR 44

Figure 10. qRT-PCR analysis of the two ZK829.4 3' UTR transcripts 50

Figure 11. Expression patterns of the *ZK829.4*$_{promoter}$::GFP:: 3' UTR constructs 53

Figure 12. Expression patterns of integrated *ZK829.4*$_{promoter}$::GFP::3' UTR strains 55

Figure 13. GDH mutations found in individuals with HI/HA (Stanley, Lieu, et al., 1998) 61

Figure 14. DAF-28::GFP expression levels in the absence and presence of the *ZK829.4(G477D)* mutant construct 64

LIST OF TABLES

Table 1. ZK829.4 Sequencing Results.....16

Table 2. GFP expression patterns of the truncated *ZK829.4*$_{promoter}$::GFP constructs.....28

Table 3. Best predicted TF binding sites from TESS for the promoter sequence between -452bp and -391bp.....30

Table 4. Expression patterns of the different ZK829.4promoter::GFP::3' UTR constructs.....52

GENERAL INTRODUCTION

The identification and characterization of *let*hal *(let*) mutations in *Caenorhabditis elegans* helps increase our understanding of the effects these mutations have on organismal development and other processes. Lethal mutations occur in essential genes, which are by definition, those genes necessary for the development or fertility or an organism. These mutations have a range of phenotypes, from blocking at the embryonic stage to adult sterility. Due to the central role essential genes play, many are evolutionarily well-conserved. In humans, mutations in many essential genes are associated with diseases. By studying these genes in model organisms with well-conserved homologs, we can easily translate the data to learn more about the human disease, or the function of the human gene. In this thesis, I focus on the molecular characterization of *let-56* in *C. elegans*.

*unc*oordinated-*22* (*unc-22*) encodes for twitchin, a large muscle protein involved in actomyosin contraction and relaxation cycles. The *unc-22 IV* region is defined by the deficiency *sDf2*, and is approximately 2 map units in length (Clark et al. 1988; Clark 1990). Previous efforts in the Baillie Laboratory at Simon Fraser University focused on the genetic and molecular characterization of this region, to study gene content and genome organization in a small, well-defined area of the *C. elegans* genome (Rogalski et al. 1982; Rogalski and Baillie 1985; Clark et al. 1988; Clark 1990; Clark and Baillie 1992; Marra 1994). One approach to the study of gene organization in the *unc-22* region was to mutationally saturate the area. *let-56* alleles were generated via treatment with

ethyl methanesulfonate (EMS) in screens for essential genes in the *unc-22* region (Moerman and Baillie 1979; Rogalski et al. 1982; Rogalski and Baillie 1985; Clark et al. 1988; Clark 1990; Marra 1994). *let-56* is intriguing because it is the largest target for EMS mutagenesis in the region, with twelve isolated alleles. There are multiple phenotypes associated with *let-56* mutants, including larval arrest, slow growth, and sterility (Clark and Baillie 1992; Marra 1994). In Chapter 1 of this thesis, I determine that the molecular identity of *let-56* corresponds to the *ZK829.4* genomic region by sequencing seven of the twelve alleles.

ZK829.4 encodes for glutamate dehydrogenase (GDH), which is highly and ubiquitously expressed in *C. elegans*. *ZK829.4* has 684 expressed sequence tags (ESTs) (http://nematode.lab.nig.ac.jp/), and the Genome B.C. *C. elegans* Gene Expression Consortium has also sequenced a large number of serial analysis of gene expression (SAGE) tags for *ZK829.4* (McKay et al. 2003). Currently, the concise description for *ZK829.4* indicates that it is orthologous to the human gene glycine decarboxylase precursor in WormBase (WS201), however, *ZK829.4* is correctly annotated as GDH in the gene model, gene ontology, and homology (WormBase, WS201).

Glutamate dehydrogenase is a mitochondrial matrix enzyme that functions as a homohexamer in its mature form. GDH catalyzes the reversible oxidative deamination of glutamate to α-ketoglutarate and ammonia, using NADP or NAD as a cofactor. Consequently, GDH plays a key role in mediating the branch point between carbon and nitrogen metabolism, and its activity is closely tied to the energy and amino acid levels of a cell. This is reflected in its allosteric effectors: GTP is an allosteric inhibitor of GDH, whereas ADP and leucine are allosteric activators (Dieter et al. 1981; Smith and Stanley

2008). This indicates that GDH activity is downregulated with energy levels are high, and upregulated when energy levels are low, or when amino acid catabolism is high. Mutations in human GDH are associated with neurodegenerative disorders such as olivopontocerebellar atrophy (OPCA), and a unique hyperinsulinism and hyperammonemia (HI/HA) syndrome (Chokroverty et al. 1990; Stanley et al. 1998). Stanley et al. (1998) determined that individuals with HI/HA were heterozygous for mutations in the GTP-binding site of GDH, indicating that loss of negative regulation by GTP is a dominant mutation that results in an overactive enzyme. Consequently, the appropriate regulation of GDH activity is fundamental to the energy requirements of a cell, and elucidating the mechanisms of GDH regulation in a simple eukaryote such as *C. elegans* can help us develop a better model to characterize the associated human diseases.

The regulation of a gene's expression or activity can occur at many levels. At the pre-transcriptional level, gene expression is controlled by chromatin structure, which dictates how available a particular locus is to the transcriptional machinery. Transcriptional regulation modulates when, where, and at what level a particular mRNA transcript is produced. It is mediated by transcription factors that bind to specific sequences, or *cis*-regulatory elements, and indirectly associate with the RNA polymerase machinery to alter the strength of promoter binding, and thus the transcription rate. At the translational level, gene expression is modified by factors that can stabilize or destabilize the mRNA transcript. For instance, microRNAs (miRNAs) are short noncoding RNAs that have sequences complementary to their target mRNAs. Through their complementarity, miRNAs results in downregulation of the mRNA message, either through direct inhibition of translation by the ribosomal machinery, or by targeting the

mRNA to be degraded. Post-translationally, there are many methods by which to modify the activity or expression of a gene. Covalent modifications such as phosphorylation, or ubiquitination, can alter activity or target a protein for degradation. Alternatively, the presence of different cofactors, activators, or repressors, can also modify the activity. By understanding the nature of a gene's regulation, we are able to learn about fundamental processes, such as how that regulation corresponds with the differentiation of cell type and fate in multicellular, complex organisms.

C. elegans represents an advantageous model in which to study the regulation of GDH at multiple levels. Its small size and short life cycle (three days at 20˚C) make it relatively easy and inexpensive to maintain, as well as to carry out experiments in a timely manner. Two sexes, hermaphrodite and male, make it simple to maintain as well as to perform genetic crosses. *C. elegans* is the first multicellular organism to have its entire genome sequenced, and the current availability of genome sequences for related *Caenorhabditis* species provides a strong tool for comparative genomics. Cross-species comparison allows for the identification of conserved regions of sequence that may have functional importance in gene regulation, and facilitates the identification of elements critical for the temporal or spatial regulation of gene expression. Furthermore, there are many genetic tools available for *C. elegans*, including established genetic markers, deficiencies, and balancers that cover almost the whole genome. RNA interference (RNAi), a powerful technique for reverse genetics was first pioneered in *C. elegans* (Fire et al. 1998). In addition, *C. elegans* is a simple eukaryote with an essentially invariant cell lineage that has been mapped from a single-celled zygote to gravid adult (Sulston et al. 1983). Its transparent body allows researchers to easily examine internal development,

and, most importantly for my study, it is especially useful for the analysis of gene expression *in vivo* using fluorescent reporter genes, such as green fluorescent protein (GFP) (Chalfie et al. 1994).

This thesis is divided into two major parts: 1. The identification of the molecular identity of *let-56* as *ZK829.4*, and determination of its lethal arrest stage (chapter 1) (described above), and 2. The study of the regulatory mechanisms of *let-56* (chapters 2, 3 and 4).

In chapter 2, I attempt to determine a possible *cis*-regulatory element in the 5' upstream region of *ZK829.4* by taking advantage of promoter driven GFP constructs. The *let-56* promoter region was sequentially truncated from the 5' end. Fragments were fused to GFP, and injected into the nematode. Transgenic strains were screened for loss of expression to identify the minimal promoter element necessary for GFP expression. In this way, I identified a 31bp window likely to contain a TF binding site necessary for transcription of *ZK829.4*.

In chapter 3, I analyze the role of the 3' UTR in mediating transcriptional regulation of *let-56* expression, since multiple miRNA binding sites are predicted to exist in this region. I generated chimeric GFP reporter constructs driven by the endogenous *let-56* promoter and fused to different 3' UTRs. I determine that the 3' UTR does play a role in regulating the level of GDH expression, and may also affect the spatial expression pattern of GDH. Also, since the *ZK829.4* gene model has two transcripts annotated for the 3' UTR, one spliced and one unspliced, that differ in their miRNA binding sites, I performed qRT-PCR analysis to determine whether they are differentially expressed

during development. I determine that the 3' UTR may also play a role in regulating the temporal expression of *let-56*.

Finally, in chapter 4 I analyze an aspect of post-translational regulation of GDH activity by the negative allosteric effector, GTP. I do this by mimicking a mutation commonly found in individuals with HI/HA (Stanley et al. 1998). As mentioned above, Stanley et al. (1998) determined that patients with HI/HA were heterozygous for mutations in the GTP-binding site of GDH, indicating that the mutation is acting dominantly. Consequently, the mutant construct was directly injected into a DAF-28::GFP background, on the basis that it would also function dominantly. DAF-28 is a beta-type insulin homologous to human insulin. From this analysis I determined that *C. elegans* GDH plays a similar functional role in regulating levels of insulin in the organism, and that its mechanism of allosteric regulation by GTP has been evolutionarily conserved.

CHAPTER 1: DETERMINATION OF THE MOLECULAR IDENTITY AND THE LETHAL ARREST STAGE OF *LET-56*

1.1 Introduction

1.1.1 The *unc-22(IV)* region and *let-56*

unc-22(IV) encodes twitchin, a large 6839 amino acid protein expressed in the muscle that regulates actomyosin contraction-relaxation cycles. Mutations in *unc-22* result in individuals with a characteristic "twitching" of the body wall musculature (Moerman and Baillie 1979). Characterization of the *C. elegans unc-22* region on chromosome *IV* has been of interest in our laboratory to further understanding of genome organization, particularly how gene arrangements or clusters may have a functional basis or may have arisen due to evolutionary constraints. The *unc-22* region is near the right end of chromosome *IV*, is defined as the interval spanned by the deficiency *sDf2*, and is roughly two map units in length (Clark et al. 1988; Clark 1990). It has been investigated at the genetic level via large scale EMS mutagenesis screens to mutationally saturate the area for all genes tightly linked to *unc-22* and essential for development (Rogalski et al. 1982; Rogalski and Baillie 1985; Clark et al. 1988; Marra 1989; Clark and Baillie 1992; Marra 1994). Genetic characterization of the *unc-22* region would lead to better estimates of the number of genes in the area, better molecular characterization of the region, and a better understanding of the gene relationships in the region. These studies resulted in the

identification of 101 lethal or sterile mutations that define 40 complementation groups mapping within *sDf2* (Marra 1994).

let-56 was one of the first essential genes uncovered in the *unc-22* region, with twelve alleles generated via treatment with EMS between 1976 and 1990 (Moerman and Baillie 1979; Rogalski et al. 1982; Clark et al. 1988; Clark 1990; Marra 1994). Molecular identification of *let-56* has been of particular interest since *let-56* is the first essential gene immediately to the left of *unc-22*, and its locus is the largest target for EMS mutagenesis in the region. Investigations at the molecular level have previously been conducted by S.S. Prasad, D.V. Clark, and M.A. Marra (Prasad and Baillie 1989; Clark and Baillie 1992; Marra 1994). To describe the isolation of *ZK829.4* as a candidate for the molecular identity of *let-56*, I have summarized their investigations here.

Prasad identified nine genes residing on the four cosmids C29E6, C11F2, C18D3, and C13G4, in the *unc-22* region via interspecies hybridization to *C. briggsae* (Prasad and Baillie 1989). Clark subsequently demonstrated that C11F2 rescues *let-56*, and C29E6 rescues *let-653*, thus defining the boundaries of the physical map in the *let-653* to *let-56* region (Clark and Baillie 1992). Molecular analysis by M.A. Marra resulted in the identification of four genes on C11F2, corresponding to *ZK822.5*, *ZK829.2*, *ZK829.5*, and *ZK829.4*. He also further refined the *let-56* region by localizing the left breakpoint of the deficiency *sDf83* within the 5' end of *ZK829.2* (Marra et al. 1993; Marra 1994). Marra also showed that *sDf83* failed to complement *let-56*, limiting candidate genes to *ZK829.2*, *ZK829.5*, and *ZK829.4*. These results were confirmed by rescue of *let-56* with a coinjection of *pCes122* and *pCeh891* (Marra 1994). The above results are summarized in Figure 1.

Genome-wide RNAi screens in *C. elegans* have made it possible to correlate lethal phenotypes with RNAi phenotypes to molecularly identify lethal genes. RNAi experiments targeting either *ZK829.2* (Kamath et al. 2003; Rual et al. 2004; Fernandez et al. 2005; Sonnichsen et al. 2005) or *ZK829.5* (Rual et al. 2004; Sonnichsen et al. 2005) showed no phenotype. RNAi against *ZK829.4* (Rual et al. 2004; Ceron et al. 2007), however, resulted in reduced brood sizes, or slow growth, or sterile adults (WormBase, WS201). Consequently, *ZK829.4* was determined to be the best candidate for *let-56*.

I determined the molecular identity of *let-56* by sequencing the *ZK829.4* genomic region in seven out of twelve alleles. Homozygous mutant individuals were first isolated and their genomic DNA obtained via single worm lysis. *ZK829.4* was then amplified via PCR, and the subsequent products sent to Macrogen Korea for sequencing. I found G-C to A-T transitions for all seven alleles, corresponding to treatment with EMS. Mutations resulted in amino acid changes in evolutionarily conserved residues, or a truncated protein in the case of *s168*. *let-56*(*s168*) individuals were also rescued with the fosmid *WRM069dG08* which covers *let-56* but not *unc-22*. Determination of the molecular identity of *let-56* provides us with greater understanding as to how mutations in this essential gene result in developmental arrest and organismal lethality.

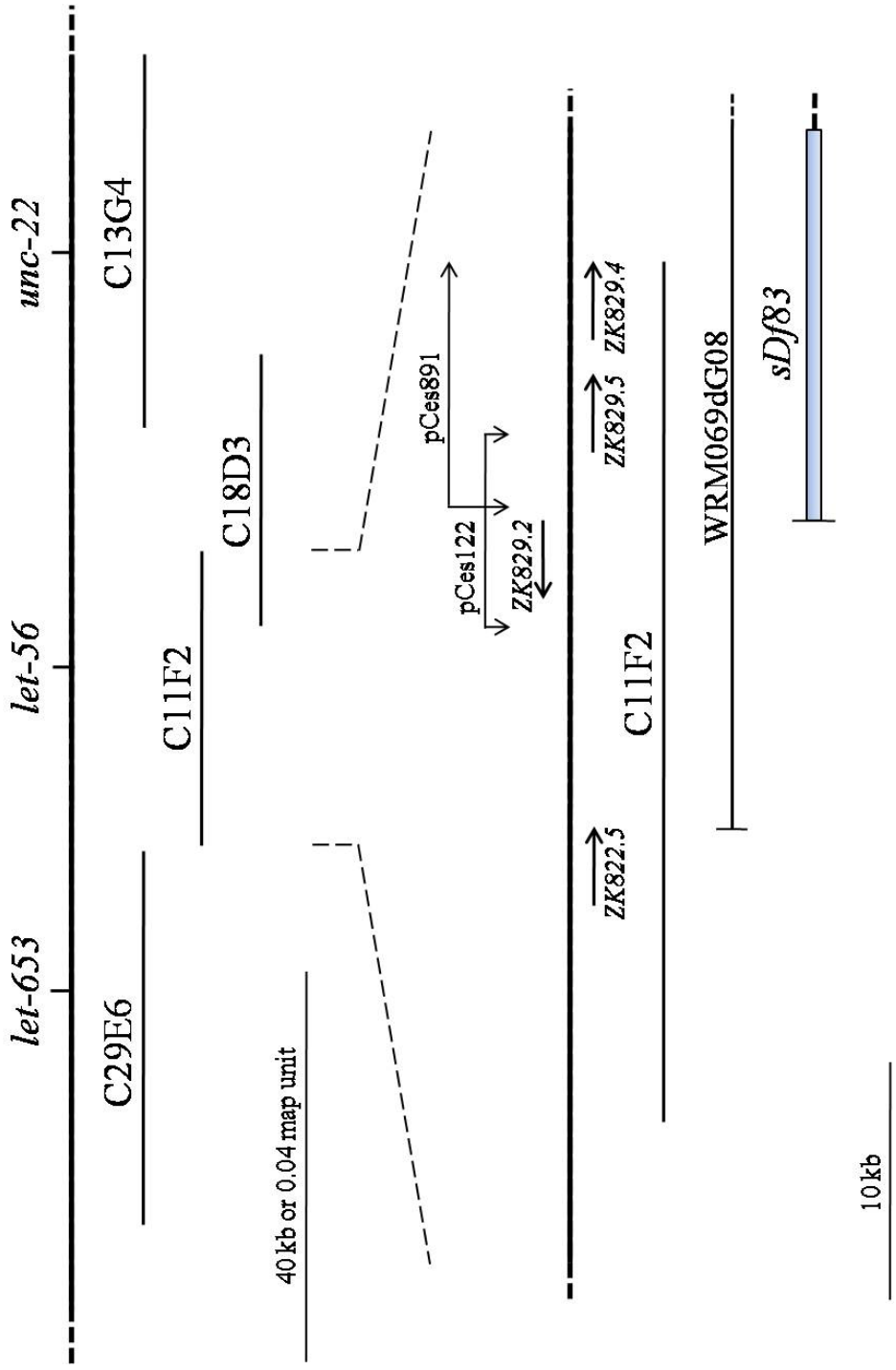

Figure 1. Isolating *let-56* candidate genes.

A summary of the correlation between the physical and genetic maps in the *let-56* region (adapted from (Clark 1990; Clark and Baillie 1992; Marra 1994)). *let-56* was rescued by the cosmid C11F2, and by coinjection of pCes122 and pCes891. *sDf83* failed to complement *let-56*, and its left breakpoint is within the 5' end of *ZK829.2*.

1.1.2 The lethal arrest stage of *let-56(s173)*

Previous work by D.V. Clark and M.A. Marra scored the lethal arrest stage of *let-56(s173)* as either mid- to late-larval lethal, or sterile adult, respectively (Clark 1990; Marra 1994). The key difference in their methodology is the basis on which the homozygous mutant organisms were scored. In her thesis, Clark measured the length of an individual three days after isolating it as a homozygous mutant at 20°C (Clark 1990). Marra, however, screened for the extent of gonadal development (Kimble and Hirsh 1979) approximately fourteen days post-egg lay at 20°C (Marra 1994). Here, I determined the lethal arrest stage of *let-56(s173)* to be early-larval two weeks after egg lay at 20˚C, using gonadal development as an indicator.

1.2 Materials and Methods

1.2.1 Nematode strains and culture conditions

Nematode strains were maintained on Easiest Worm Plate Agar streaked with *Escherichia coli OP50* (Brenner 1974). The wildtype strain used was N2 (var. Bristol, Baillie Laboratory strain, BC49). The strains used in this study had the genotype *let-56(s-x) unc-22(s7)/nT1(IV);+/nT1(V)[let- (m435)* on *nT1]* or *let-56(s-x) unc-22(s7) lev-1(x22)/nT1(IV);+/nT1(V) [let- (m435)* on *nT1]*. Specific *let-56* alleles characterized were: *s46, s50, s168, s173, s1192, s1223,* and *s2230*. For the list of *let-56* strains analyzed via sequencing, refer to Appendix A.

1.2.2 Isolation of homozygous *let-56* individuals

Thirty gravid hermaphrodites for each *let-56* strain were selfed and allowed to lay eggs for two three-hour broods at 20°C. *let-56* homozygous mutants have previously

been characterized as either mid- to late-larval arrests (Clark 1990), or as slow-growing sterile adults (Marra 1994). Viable progeny were removed from the plate as they matured, until only developmentally arrested individuals remained. Since all strains were balanced over *nT1 [let- (m435)]*, all developmentally arrested individuals isolated were *let-56* homozygotes since *nT1* homozygotes are embryonic lethal.

1.2.3 Isolation of *C. elegans* genomic DNA

Genomic DNA was isolated from organisms via single worm lysis. One worm was picked for every 2µl of lysis buffer, and 1µl of the genomic DNA was then used as template for a 20µl PCR reaction.

1.2.4 *ZK829.4* PCR amplification and sequencing

Wildtype sequence for the *ZK829.4* genomic region was obtained from WormBase (WS170). All primers were designed using Primer3 (Rozen and Skaletsky 2000). *ZK829.4* PCR amplification primers: forward: `gccta gaagc gtttg cctac t`, nested forward: `agacc tcctg gcatt ttcct`, reverse: `gccaa gcatc aactt cgttt a`, nested reverse: `aaagt tttta atgct ccctg aaa`. Sequencing primers were designed every 500bp, staggered on either strand. For the wildtype *ZK829.4* sequence and a list of the sequencing primers used, refer to Appendix B. Samples were sent to Macrogen Korea for sequencing.

1.2.5 Sequence analysis

Sequence results were analyzed for nucleotide mutations, and corresponding amino acid changes using BioEdit (http://www.mbio.ncsu.edu/BioEdit/BioEdit.html), a biological sequence alignment editor. The extent of conservation between amino acid

sequence alignments for different species were visualized using GeneDoc (http://www.psc.edu/biomed/genedoc).

1.2.6 Microinjection

Transgenic organisms containing the fosmid *WRM069dG08* were created via microinjection directly into the syncitium of the nematode gonad. Microinjection needles were made from 1.0-mm, 6" filamented capillary tubes (World Precision Instruments) using a Sutter P-97 horizontal needle puller, and were mounted into a Leitz Wetzlar micromanipulator. All microinjections were conducted by Domena K. Tu, using either an Olympus BH2-HLSH or a Zeiss 47 3016 inverted microscope. *dpy-5/dpy-5* worms were mounted atop dry agarose pads on 48 x 65mm microscope cover slips (Gold Seal Cover Glass, reorder number 3335) using mineral oil (Sigma, M-3516). *WRM069dG08* was injected at a final concentration of 3ng/µl, along with *pCeh361* (a *dpy-5* rescue construct) at 100ng/µl, and *myo-2::GFP* (a GFP marker driven by the *myo-2* promoter, which expresses in the pharynx, and the first and second pharyngeal bulbs) at 10ng/µl. Injected P_0s were arranged 5 per plate. Phenotypically wildtype F_1s were plated two-per-plate and allowed to self. Wildtype F_2 lines expressing GFP and containing the fosmid (see 1.2.7 Fosmid PCR check) were selected to establish a transgenic line, and only one F_2 line was retained per original P_0 plate. If more than one P_0 plate generated a stable F_2 line, it was retained as an independent segregant. Fosmid strain generated: BC7780; seX1682 *dpy-5(e907)/dpy-5(e907) [WRM069dG08+pCeh361+myo-2::GFP]*.

1.2.7 Fosmid PCR check

PCR primers specific to the fosmid backbone were designed by ShuYi Chua. Fosmid-F: `gcgac cacgt tttag tctac g`, Fosmid-R: `tcaat acttg ccctt gacag g`.

1.2.8 Rescue of *let-56* with fosmid *WRM069dG08*

The fosmid *WRM069dG08* covers *ZK829.4* but not *unc-22*, and thus was chosen to rescue *let-56(s168). s168* was chosen since its mutation results in a truncated protein, and therefore constitutes a null allele. *WRM069dG08* was introduced into *C. elegans* via microinjection (see 1.2.6 Microinjection). *dpy-5(e907)/dpy-5(e907) [WRM069dG08+myo-2::GFP+pCeh361]* individuals were crossed to +/+ N2 males to obtain *dpy-5(e907)/+ [WRM069dG08+myo-2::GFP+pCeh361]* males. These GFP-expressing males were then crossed to *let-56(s168) unc-22(s7)/nT1(IV);+/nT1(IV) [let-(m435)* on *nT1]* hermaphrodites. F_1 progeny were screened for the presence of males to ensure that crossing had occurred. Wildtype F_1 hermaphrodites were individually plated and allowed to self. F_2 progeny were screened for the presence of unconditional twitchers of the genotype *let-56(s168) unc-22(s7)/let-56(s168) unc-22(s7)(IV) [WRM069dG08+ myo-2::GFP+pCeh361]*. Unconditional twitchers were individually plated and incubated at 20°C for 5 days to screen for full rescue (presence of progeny) or partial rescue (no progeny). *s168* individuals were fully rescued and a line was maintained: (BC7861; sEX1682) *let-56(s168) unc-22(s7)/let-56(s168) unc-22(s7)(IV) [WRM069dG08+myo-2::GFP+pCeh361]*.

1.2.9 Determination of *let-56(s173)* lethal arrest stage

Forty gravid nematodes of the genotype *let-56(s173) unc-22(s7)/nT1(IV); +/nT1(V) [let- (m435)* on *nT1]* were selfed and allowed to lay eggs for four two-hour broods at 20°C. Viable progeny were removed from the plate as they matured, until only developmentally arrested individuals remained. *let-56* homozygotes were maintained at 20°C for two weeks post-egg lay before screening for extent of gonadal development (Kimble and Hirsh 1979; Marra 1994). The screen for lethal arrest stage was done on both easiest worm plate agar and nematode growth media (NGM).

1.2.10 Microscopy

The extent of *let-56(s173)* homozygote gonadal development was screened using a Zeiss Axioscope equipped with a QImaging camera. Nematodes were immobilized on moist 2% (in water) agarose pads using 1mM levamisole (in M9) (Sigma, L9756-5G) immediately prior to imaging. Images were captured under identical lens and camera settings, using QCapture software, and were processed using Adobe Photoshop CS.

1.3 Results

1.3.1 Sequencing results

All seven *let-56* alleles analyzed had a G-C to A-T transition, corresponding to treatment with EMS. In the *s46*, *s50*, *s173*, *s1192*, *s1223*, and *s2230* alleles, the nucleotide transition resulted in a significant amino acid change, such as glycine to glutamic acid, in a well-conserved residue. The *s168* mutation had the most severe allele, with a prematurely truncated protein at 73 amino acids. Nucleotide changes and their corresponding amino acid mutations for each allele are summarized in Table 1.

1.3.2. Rescue of *let-56(s168)* with the fosmid *WRM069dG08*

Since *s168* most likely represents a null allele, it was chosen as a candidate for rescue. The fosmid *WRM069dG08* was chosen to rescue *let-56* since it covers the *ZK829.4* genomic region, but not the *unc-22* gene. *WRM069dG08* was introduced into *C. elegans* via microinjection along with *myo-2::GFP* as a marker. GFP-expressing males were generated by crossing the resulting transgenic strain to wildtype N2 males, and were then crossed to *let-56(s168)* hermaphrodites. GFP-expressing F_1s were plated individually, and their progeny screened for viable *let-56(s168)* homozygotes of the genotype *let-56(s168) unc-22(s7)/let-56(s168) unc-22(s7)(IV) [WRM069dG08+myo-2::GFP+pCeh361].* These individuals were isolated based on their characteristic "twitching" body wall musculature. *let-56(s168)* individuals were fully rescued by *WRM069dG08*, giving rise to fertile progeny. A line was retained and designated as BC07862 (sEX1682).

Table 1. ZK829.4 Sequencing Results

***let-56* Allele**	**Nucleotide change**	**Amino acid mutation**
s46	G795A	Gly235Arg
s50	G1020A	Glu310Lys
s168	C217T	Gln73Stop
s173	G1012A	Gly307Glu
s1192	G1252A	Gly387Glu
s1223	C586T	Thr180Ile
s2230	G519A	Gly158Glu

1.3.3. The lethal arrest stage of *let-56(s173)*

Previous screens to determine the lethal arrest phase phenotype of *let-56* by D.V. Clark and M.A. Marra yielded different results. By scoring the length of each homozygous mutant 3 days post-isolation at 20°C, Clark determined that *let-56* individuals arrest as mid- to late-larvae (Clark 1990). However, by screening for the extent of gonadal development 14 days post-egg lay at 20°C, Marra determined that *let-56* individuals arrest as smaller, sterile adults (Marra 1994). Since gonadal development is a better indicator of maturity than organismal length, I have screened for the lethal arrest stage of *let-56(s173)* following M.A. Marra's protocol. *let-56(s173)* was chosen since it was the earliest arresting allele analyzed by Clark (1990), reportedly arresting at the mid-larval stage, and was also analyzed by Marra (1994) and found to attain sterile adulthood. I scored 42 homozygous *s173* individuals and found that all of them arrested as early-larval lethals based on the extent of their gonadal development (Figure 2).

1.4 Discussion

Based on sequencing results of the *ZK829.4* region in seven of twelve *let-56* alleles, and on rescue of *s168* lethality by *WRM069dG08*, I conclude that *ZK829.4* is the molecular identity of *let-56*.

ZK829.4 encodes for glutamate dehydrogenase (GDH), a homohexameric mitochondrial matrix enzyme that catalyzes the reversible oxidative deamination of glutmate to α-ketoglutarate and ammonia using NADP or NAD as a cofactor. Glutamate plays numerous physiological roles within an organism. Besides being a building block for proteins, glutamate can also act as a neurotransmitter, it is a metabolic intermediate of the tricarboxylic acid (TCA) cycle, an intracellular messenger, and is also necessary for

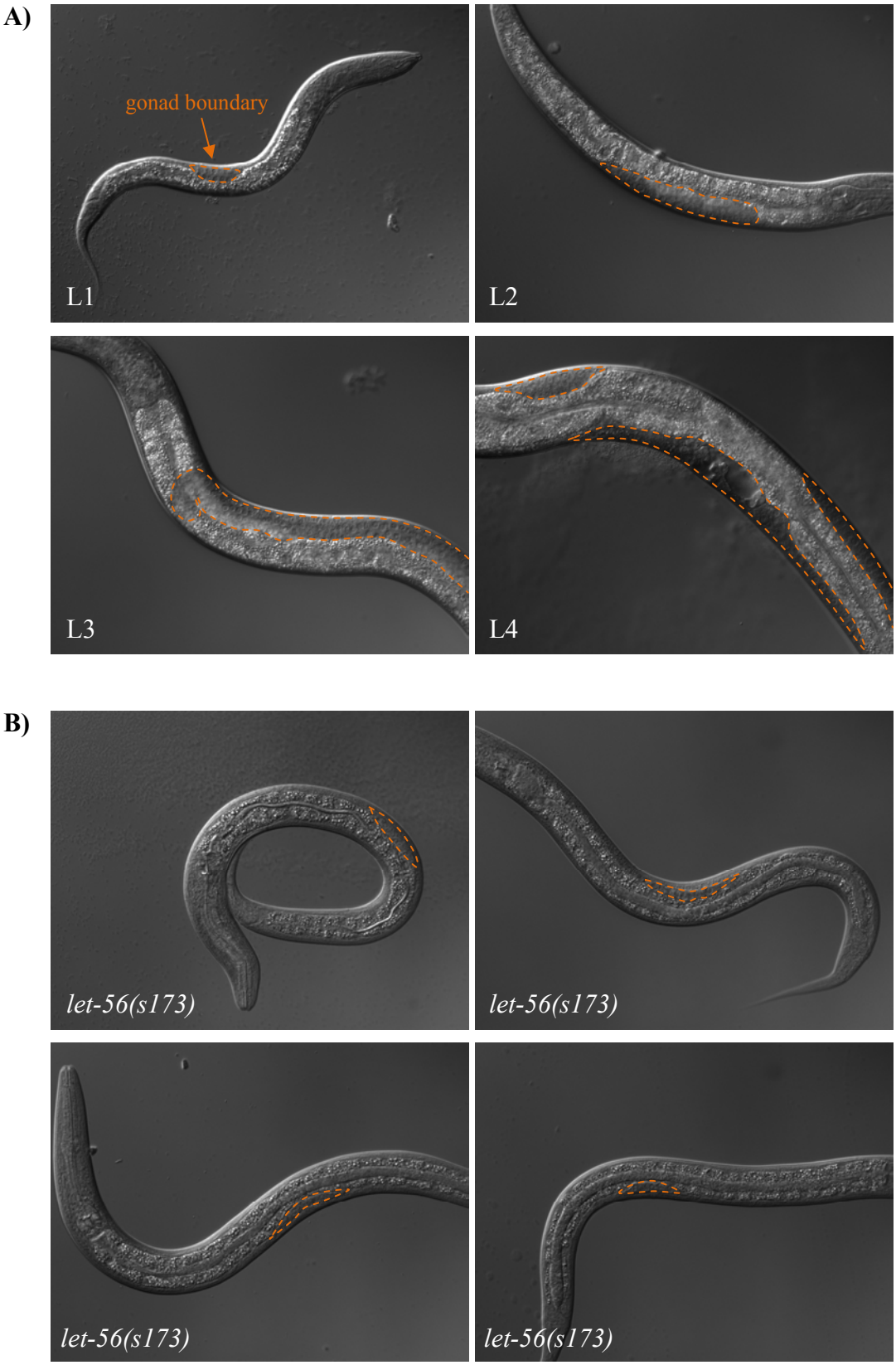
A)
gonad boundary
L1
L2
L3
L4
B)
let-56(s173)
let-56(s173)
let-56(s173)
let-56(s173)

Figure 2. Extent of gonadal development in *let-56(s173)* homozygotes

A) Extent of gonadal development in wildtype (N2) larvae at the mid- L1, L2, L3, and L4 stages. In L1 hermaphrodites, the gonad divides to contain 12 cells, after which it starts to elongate anteriorly and posteriorly during the L2 stage. By L3, the gonadal arms start to turn 180˚, and by L4 they are elongating in the opposite direction to form the U-shaped ovitestis structure. (Hirsh et al. 1976; Kimble and Hirsh 1979)

B) Extent of gonadal development in *let-56(s173)* homozygotes after two weeks at 20˚C. Gonads appear to be roughly equivalent in size to those of late-L1 to early-L2 wildtype larvae, indicating that *let-56*(*s173*) homozygotes arrest at an early larval stage.

Orange borders indicate gonad boundaries.

ammonia metabolism (Frigerio et al. 2008). GDH activity plays a key role in regulating the levels of glutamate inside the cell, as well as in modulating the amount of α-ketoglutarate available to undergo the TCA cycle. Consequently, it occupies a pivotal position mediating the branch point between carbon and nitrogen metabolism (Frigerio et al. 2008). Due to the importance of its function, it is unsurprising that GDH is found in almost all living organisms and that it is evolutionarily well conserved, with 56.3% identity and 69.7% similarity between the human and *C. elegans* proteins (pairwise alignment). Six out of seven of the identified G/C to A/T transitions resulted in significant amino acid changes in highly conserved residues, with the seventh mutation resulting in a truncated protein (Figure 3).

A GDH monomer is generally 450 to 550 amino acids long and consists of multiple functional domains. It has a catalytic cleft, an NAD (or coenzyme) binding domain, a multimerization domain, and an 'antenna' that is necessary for allosteric regulation of GDH (Smith and Stanley 2008). Considering the number of domains and the extent of evolutionary conservation, it is understandable that *let-56* is a large target for mutagenesis. The majority of the identified *let-56* mutations are found close to the catalytic cleft (*s46*, *s1192*, *s2230*), or within the NAD binding domain (*s50*, *s173*), with the other mutations being found in the multimerization domain (*s1223*) or resulting in a 73-AA truncated protein (*s168*).

Defects in human GDH have been associated with a unique hyperinsulinism and hyperammonemia (HI/HA) syndrome (Stanley et al. 1998), as well as with forms of cerebellar degeneration such as olivopontocerebellar atrophy (OPCA) (Chokroverty et al. 1990). In *C. elegans* the *let-56* mutations have been associated with mid- to late-larval

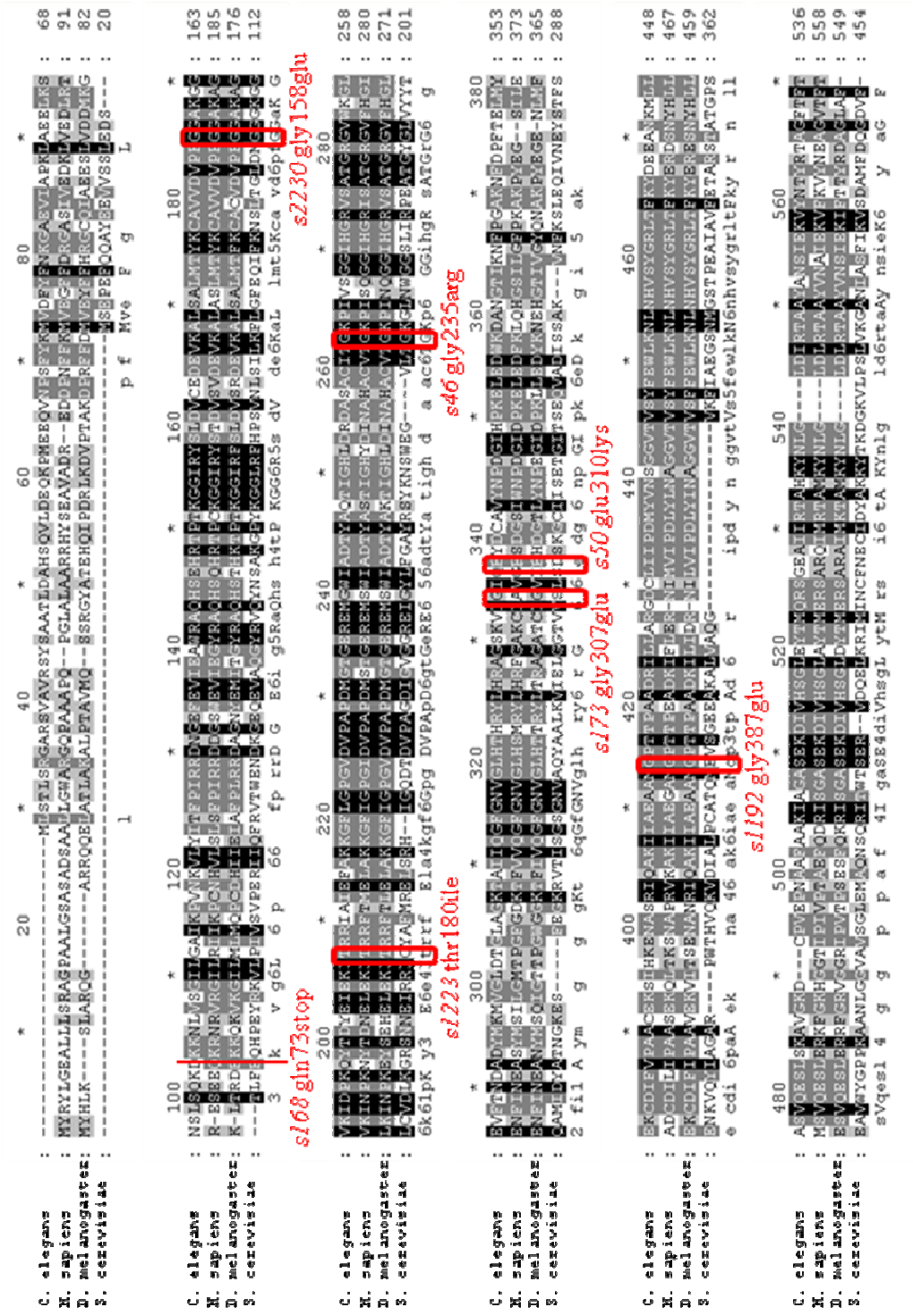

Figure 3. GDH conservation and location of identified AA mutations in let-56 alleles

GDH is evolutionarily highly conserved, with 56.3% identity between the human and *C. elegans* proteins. *let-56* mutations generally occur in well conserved residues.

arrest, or slow growth and sterility (Clark 1990; Clark and Baillie 1992; Marra 1994). Wildtype nematodes have a lifecycle of approximately 3 days at 20˚C, with an individual first being able to lay eggs 59-60 hours post-hatching (Hirsh et al. 1976). Using animal length as an indicator, Clark previously determined that *let-56(s173)* homozygotes arrest at the mid- to late-larval stage (Clark 1990; Clark and Baillie 1992). However, when Marra used gonadal development as an indicator, he determined that *s173* individuals arrest as smaller, sterile adults after two weeks at 20°C (Marra 1994). In a similar screen I determined the arrest stage for *s173* individuals to correspond to early-larval lethality after 14 days at 20˚C (Figure 2). One possibility I examined to account for the difference in arrest stage was the media on which the strains were maintained. Marra used nematode growth media (NGM), whereas I used easiest worm plate agar. Easiest worm plate agar contains approximately 20% more peptone and 40% more cholesterol, whereas NGM contains roughly 30% more NaCl. However, when I repeated the screen with NGM, no difference in arrest stage was seen between *s173* individuals raised on either media. Another possible explanation for the observed difference in arrest stage is the accrual of additional mutations in the *s173* strain used for my screens, which have additionally slowed their growth or exacerbated the lethal phenotype. It is possible that these *s173* homozygotes need greater than 2 weeks at 20˚C to attain adulthood. Additional screens would need to be carried out with longer wait times to ascertain whether *s173* individuals can reach adulthood. In addition, determination of the lethal arrest stage for all the available *let-56* alleles would provide more conclusive results as to the lethal arrest stage of *let-56*.

CHAPTER 2: IDENTIFICATION OF A 5' *CIS*-ACTING REGULATORY MOTIF IN THE PROMOTOR REGION OF *ZK829.4*

2.1 Introduction

Non-coding DNA sequences can play key regulatory roles in gene expression. For instance, gene intronic regions contain sequences necessary for the correct splicing of exons. Activators and repressors, generally referred to as transcription factors, can bind to *cis*-regulatory elements and indirectly modify the strength of association between RNA polymerase and the promoter. In this way, *cis*-regulatory elements work at the transcriptional level to help modulate the spatiotemporal expression of a gene during development. Studying these elements can provide us with insights into fundamental mechanisms, such as cell differentiation or tissue specificity in multicellular organisms. In addition, from the identification of a set of genes controlled by a particular *cis*-regulatory element we gain further knowledge on the functional relationships between co-regulated genes. In this section of the thesis, I attempt to identify a 5' *cis*-acting regulatory motif necessary for the transcriptional expression of GDH in the region immediately upstream of *ZK829.4*, which I define as the promoter.

To identify a *cis*-regulatory element in the promoter of *ZK829.4*, I took advantage of promoter::GFP reporter constructs, which can be easily visualized in *C. elegans* due to the transparent nature of the nematode. Due to the complex nature of the expression

pattern of GDH (pharynx, pharyngeal bulbs, gut, muscle, etc.), my study focuses simply on complete loss of GFP expression rather than changes in expression intensity, or loss of expression from some tissue types. This simplification was necessary in order to identify a minimal element necessary for GDH expression, and to avoid complications arising from tissue-specific regulatory elements. By systematically truncating the length of the promoter region fused to GFP, I was able to identify a 31bp region suspected to contain a *cis*-regulatory element necessary for expression of *ZK829.4*.

2.2 Materials and Methods

2.2.1 Construction of *let-56*$_{promoter}$::GFP transgenes

let-56$_{promoter}$::GFP constructs were generated via fusion PCR (Hobert 2002). To ensure fidelity of the constructs, Phusion polymerase (Finnzymes, New England Biolabs Cat: F530) was used for all PCRs. Promoter regions were amplified off of N2 genomic DNA (Bristol, Baillie Laboratory strain, BC49). GFP was amplified off of the *pPD95.67 (GFP)* coding cassette. *pPD95.67* contains five artificially derived introns, a 5' nuclear localization sequence (NLS) from the virus SV40, and a 3' untranslated region (UTR) from the *C. elegans unc-54* gene. Primers used for amplification of the GFP reporter are: GFP-C: `AGCTT GCATG CCTGC AGGTC GACT`, and GFP-D*: `GGAAA CAGTT ATGTT TGGTA TATTG GG` (designed by Allan K. Mah). To stitch the two PCR products together, the reverse primer for the promoter region had additional sequences complementary to the GFP-C primer. Sequences used for *let-56* promoter primer design were obtained from WormBase (WS170). The reverse primer used to amplify all of the *let-56* promoter regions was: ZK829.4-R: `AGTCG ACCTG CAGGC ATGCA AGCTG`

AAAGA GTGCT CAACA TTACC TGA. For a list of forward primers used to amplify the *let-56* promoter and their distance upstream of the ATG start site, refer to Appendix C.

The longest promoter length used for analysis was 1101bp. This construct was previously generated in an effort to determine the expression profiles of all *C. elegans* genes with human orthologs, to better understanding of gene regulatory networks (McKay et al. 2003). A longer construct was not used because the gene immediately upstream of *ZK829.4*, *tbx-36* (*ZK829.5*), is only 1167bp away.

2.2.2 Microinjection

See section 1.2.6 Materials and methods for a complete description of microinjection. All injections were done by Domena K. Tu. *let-56*$_{promoter}$::GFP constructs were injected at final concentrations of approximately 3ng/µL. All constructs were coinjected with *pCeh361* at 100ng/µL. When possible, multiple segregants for each construct were retained. When GFP expression was not seen, PCRs were conducted using GFP-specific primers and the genomic DNA of transgenic organisms to ensure lack of fluorescence was due to loss of expression driven by the promoter rather than lack of transgene uptake by the nematode. GFP-specific primers were designed by Carrie L. Simms: GFP-F: CCATG CCCGA AGGTT ATGTA, and GFP-R: AAAGG GCAGA TTGTG TGGAC. Refer to Appendix D for a complete list of strains generated in this section.

2.2.3 Microscopy

See section 1.2.10 Microscopy for a detailed description on microscopy. GFP expression pattern analysis was done using a Zeiss Axioscope equipped with a QImaging

camera and the appropriate GFP filter. All GFP images were taken under identical filter, lens, and camera settings. Exposure times are indicated on the figures.

2.2.4 Comparison of the *ZK829.4* promoter to its *C. briggsae* orthologous region

-1167bp to +50bp promoter sequences for *C. elegans ZK829.4* and its orthologous sequence in *C. briggsae* (CBG6199) were obtained from WormBase (WS198). Pair-wise alignment of the sequences was done using BioEdit, with default parameters. Alignments were viewed using GeneDoc. Refer to Appendix E for the raw sequences.

2.2.5 *Cis*-regulatory element prediction

Putative binding site prediction was done using the Transcriptional Element Search Software (TESS) (http://www.cbil.upenn.edu/cgi-bin/tess/tess), which identifies binding sites based on positional weight matrices from the TRANSFAC, JASPAR, IMD, and CBIL-GibbsMat databases.

2.3 Results

2.3.1 Sequential *let-56*$_{\text{promoter}}$::GFP deletion constructs

The initial promoter constructs used to assay GFP expression were from positions -1101bp, -593bp, -543bp, -445bp, -414bp, -363bp, and -78bp to position +17bp relative to the *ZK829.4* translational start site (TSS). For the -1101bp and -593bp to +17bp fragments, GFP expression was seen in the pharyngeal bulbs, pharynx, hypoderm, muscle, gut, anterior neurons, and the excretory cell (Figure 4). Initially, complete loss of GFP expression was seen in the -543bp to +17bp fragment, as well as in the -414bp, and -363bpto +17bp fragments. Lower levels of GFP expression were regained in the gut,

hypoderm, and anterior neurons for the -445bp to +17bp fragment (faint expression seen at ~750ms of exposure, versus ~100ms for the -1101bp and -593bp to +17bp fragments). Extremely faint GFP expression was detected in the gut of nematodes containing the -78bp to +17bp fragment. PCRs using GFP-specific primers confirmed the presence of GFP in the transgenic organisms containing the -543bp, -414bp, and -363bp to +17bp fragments. Consequently, the 50bp interval between -593bp and -543bp was chosen for a finer deletion analysis based on complete loss of GFP expression from one fragment to the next, and was cut down every 5bp.

All eight new fragments (-588bp, -583bp, -578bp, -573bp, -563bp, -558bp, -553bp, and -548bp to +17bp) expressed GFP in all, or the majority, of the tissues (the -568bp to +17bp fragment was injected multiple times, but I was unable to isolate a stable transgenic strain). The -543bp to +17bp fragment was also reinjected, since the original strain was accidentally lost. Interestingly, the new transgenic line containing the reinjected -543bp to +17bp fragment expressed GFP in most of the tissues (Table 2). Based on the current expression data, it seems that the minimal *ZK829.4* promoter element necessary for GFP expression is 445bp, with complete loss of expression seen with the -414bp to +17bp promoter fragment.

The level of GFP expression varied between the different strains, with the brightest expression being seen in the -548bp and -553bp to +17bp fragments, followed by the -1101bp, -593bp, and -588bp to +17bp fragments, followed by the -583bp and -573bp to +17bp fragments, followed by the -578bp, -563bp, -558bp, and -543bp to +17bp

Table 2. GFP expression patterns of the truncated *ZK829.4*$_{promoter}$::GFP constructs

Tissue	-1101	-593	-588	-583	-578	-573	-563	-558	-553	-548	-543	-445	-414	-363	-78
Gut	+	+	+	+	+	+	+	+	+	+	+	+	-	-	+/-
Anterior neurons	+	+	+	+	+	+	+	+	+	+	+	+	-	-	-
Hypoderm	+	+	-	+	+	+	-	+	+	+	+	+	-	-	-
Pharynx	+	+	+	+	+	+	+	+	+	+	+	-	-	-	-
Pharyngeal bulbs	+	+	+	+	+	+	+	+	+	+	+	-	-	-	-
Muscles	+	+	+	+	+	+	+	+	-	+	-	-	-	-	-
Excretory cell	+	+	-	-	+	+	-	+	+	+	+	-	-	-	-

Negative numbers along the top row indicate the position of the promoter fragment relative to the translational start site in basepairs. (+/-) indicates an extremely low level of GFP expression.

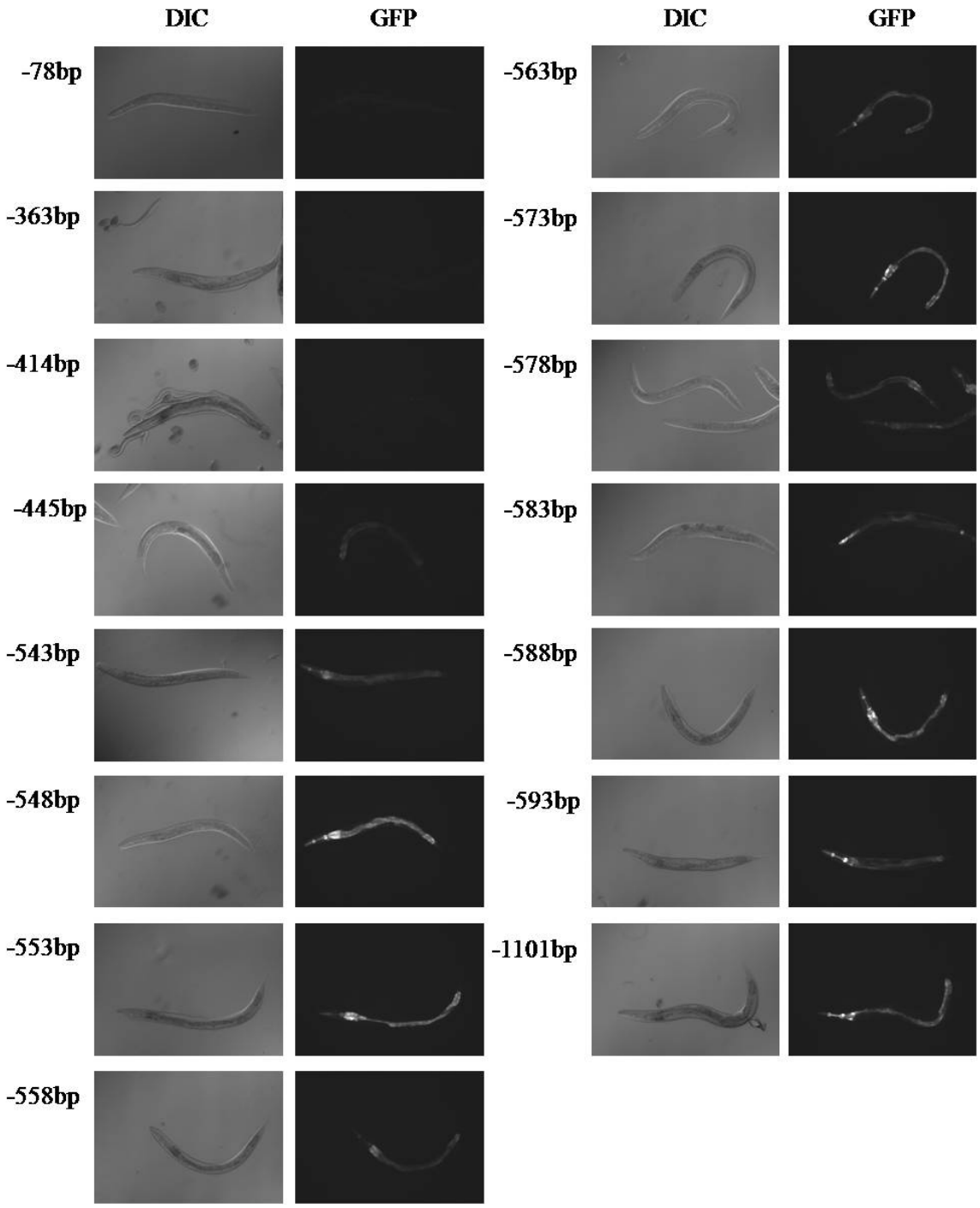

Figure 4. GFP expression levels of the different *ZK829.4*$_{promoter}$::GFP constructs

GFP expression levels varied across the different promoter::GFP constructs, with the -548bp and -553bp to +17bp fragments displaying the highest level of GFP, and the -78bp to +17bp fragment displaying the lowest (cannot be seen at 1s of exposure). All GFP images were taken at 1s exposures. Nematodes imaged were young adults to ensure similar levels of transgene expression.

fragments, followed by the -445bp to +17bp fragment, and lastly, followed by the -78bp to +17bp fragment (Figure 4). For a complete series of pictures taken at different exposure times, please see Appendix F.

2.3.2 Predicted *cis*-regulatory elements between -445bp and -414bp

The DNA sequence between positions -452bp and -391bp relative to the TSS was inputted into TESS, since there are two blocks of well conserved sequence between *C. elegans* and *C. briggsae* in this region (Figure 5). The best TF binding site predictions from TESS are displayed in Figure 5. The three strongest hits were for STE12 binding the sequence AGTTTCAT on the antisense strand, GATA-1 binding CTATCT on the sense or antisense strands, and Sp1 (specificity protein 1) binding CCCAC on the antisense strand (see Table 3 for a summary of the top predicted TF binding sites).

Table 3. Best predicted TF binding sites from TESS for the promoter sequence between -452bp and -391bp

Transcription Factor	Sense (N/R)	Sequence	La	La/	L Pv
STE12	R	AGTTTCAT	16.00	2.00	0
	N	ATGAAAC	12.61	1.80	0.0067
	R	GTTCAT	12.61	1.80	0.0067
	N	TGAAAC	11.02	1.84	0.027
	R	GTTTCA	11.02	1.84	0.027
GATA-1	N	CTATCT	12.00	2.00	0
	R	CTATCT	12.00	2.00	0
	R	YTATCW	10.00	1.67	0
Sp1	R	CCCAC	12.00	2.00	0

Sense: N – normal, R – reverse complement
La: Log-likelihood score, higher is better
La/: La/length, higher is better, maximum is 2.0
L Pv: Approximate p-value for La score

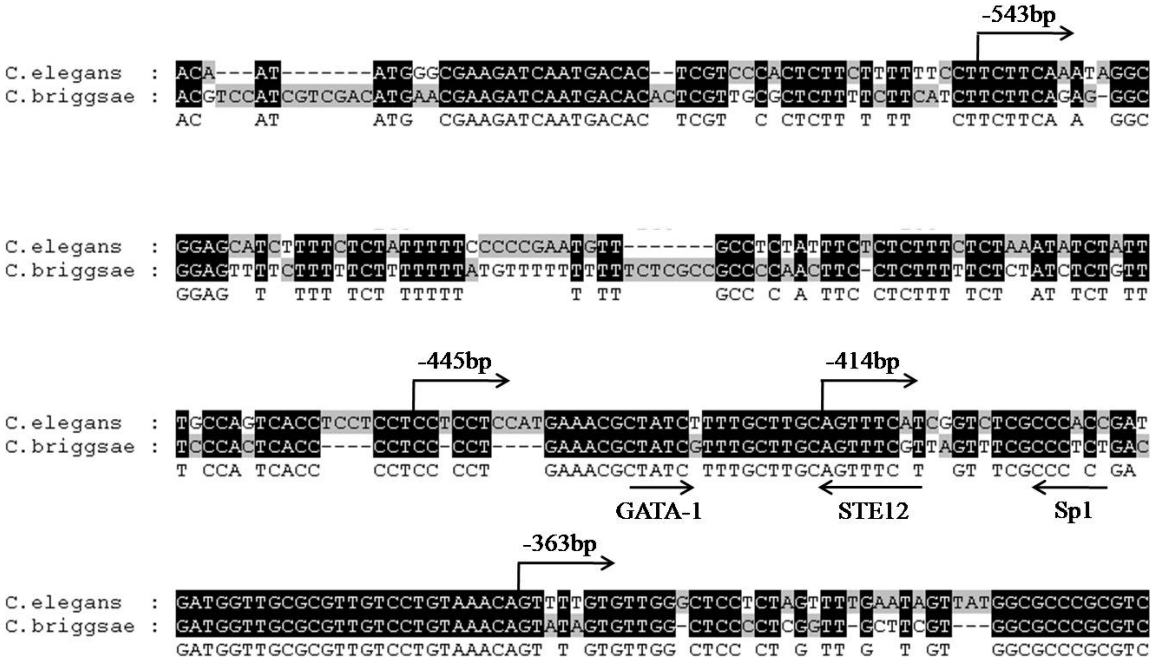

Figure 5. Sequence between -452bp and -391bp entered into TESS

Pair-wise alignment between *C. elegans* and *C. briggsae* for the promoter sequence between positions -452bp and -391bp relative to the *C. elegans* TSS. These 61 basepairs were entered into TESS, and the three best predicted TF binding sites are displayed in the figure (GATA-1, STE-12, and Sp1). (Alignment was viewed using GeneDoc).

2.4 Discussion

At the transcriptional level, gene expression can be controlled by the action of transcription factors that bind to specific sequences, or regulatory elements, in the gene. Transcription factor binding indirectly modifies the strength of the association RNA polymerase has with its promoter binding site, thus altering the level of mRNA production. Modulation of gene expression levels by TFs can be both spatial and/or temporal. Consequently, the identification of these regulatory elements can provide us with an initial understanding of gene function and mechanisms of cell differentiation. In addition, determination of a set of genes controlled by a specific TF can also provide us with greater knowledge of the genes involved in specific processes. To identify a *cis*-regulatory motif that drives expression of *ZK829.4*, I performed promoter::GFP truncations and looked for the minimal promoter construct that could still drive GFP expression.

The initial promoter fragments tested were from positions -1101bp, -593bp, -543bp, -445bp, -414bp, -363bp, and -78bp to +17bp relative to the translation start site (TSS) (initiator ATG is +1). The -78bp construct had faint GFP expression in the gut, which is most likely an artifact of the GFP reporter construct. Non-specific fluorescence has occasionally been observed in gut cells, and it is thought to be indirectly a consequence of the *unc-54* 3' UTR used in the *pPD95.67* expression cassette (Boulin et al. 2006). Initially, complete loss of GFP expression was seen from $ZK829.4_{promoter(-593)}$::GFP to $ZK829.4_{promoter(-543)}$::GFP, indicating that the regulatory sequence of interest for GDH expression lies near the 50bp stretch between these constructs. GFP expression

also returned at a lower intensity in fewer tissues with the -445bp to +17bp promoter fragment (Figure 4).

I focused on the 50bp region between -593bp and -543bp, fine tuning it by truncating the promoter every 5bp to determine the exact site necessary for gene expression. Eight additional promoter::GFP constructs were generated, starting at positions -588bp, -583bp, -578bp, -573bp, -563bp, -558bp, -553bp, and -548bp relative to the TSS. These constructs expressed GFP in most or all of the tissues (Table 2), at variable levels (Figure 4, Appendix F). Although lack of expression in some of the tissues for a few of these constructs could be due to loss of a tissue-specific regulatory element, it seems unlikely. Since loss of GFP is noticed only for the hypoderm, excretory cell, or muscle in these strains (Table 2), it is possible that GFP expression is too low in these tissues to be detected over the strong fluorescence expressed in the gut and the pharynx. Alternatively, since somatic loss of extrachromosomal DNA arrays is observed in transgenic nematodes (Herman 1984), another possibility is that not enough worms were screened for these strains to find a nematode with expression in the hypoderm, excretory cell, or muscle. Variability in GFP expression levels between strains could also be due to random somatic loss, or to inconsistencies in copy number. The concatamerization of injected DNA into an extrachromosomal array in *C. elegans* is a random process that can vary between injections. Differences in copy number would also account for the differences in GFP expression levels seen between segregants containing the same *ZK829.4*$_{\text{promoter}}$::GFP transgene (Figure 6).

A)

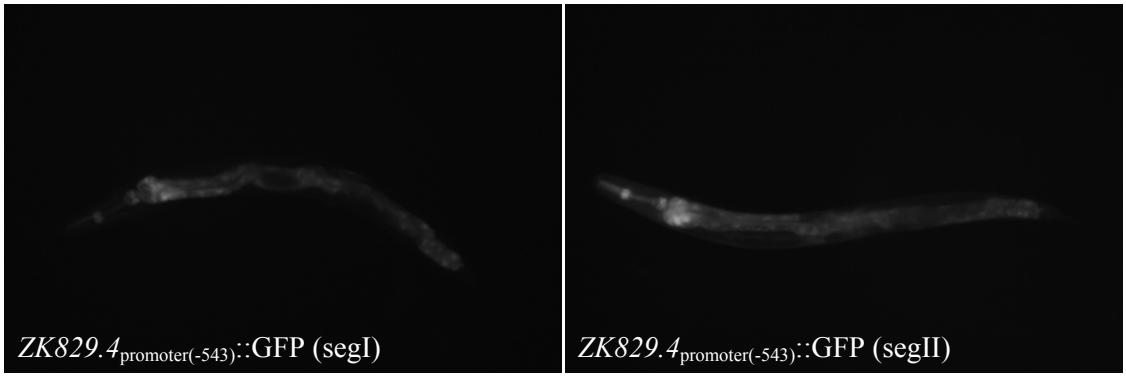

B)

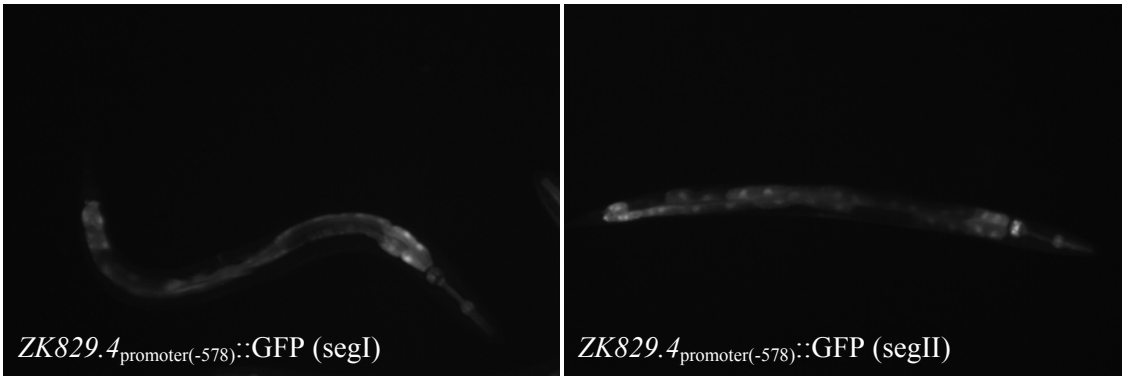

Figure 6. Differences in GFP expression levels between segregant strains with the same promoter::GFP fusion

When possible, multiple individually derived segregants were retained for each promoter::GFP injection. Differences in GFP expression levels were seen between these segregants. A) *ZK829.4*$_{\text{promoter(-543)}}$::GFP segregants I and II. B) *ZK829.4*$_{\text{promoter(-578)}}$::GFP segregants I and II. All pictures were exposed for 1500ms.

Reinjection of the -543bp to +17bp fragment showed that it is able to drive GFP expression in most of the same tissues as the *ZK829.4*$_{\text{promoter(-1101)}}$::GFP and *ZK829.4*$_{\text{promoter(-593)}}$::GFP constructs (Table 2), indicating that the site of interest may lie between -445bp and -414bp relative to the TSS. Inability to see GFP expression when the *ZK829.4*$_{\text{promoter(-543)}}$::GFP construct was first injected could be due to low transgene copy number. As mentioned earlier, the germline transformation process in *C. elegans* is still not well understood; how the nematode is able to uptake multiple segments of DNA, assemble it into a concatamer, and stably propagate that array is unknown. It is possible that individuals from the first *ZK829.4*$_{\text{promoter(-543)}}$::GFP transgenic strain isolated had enough copies of the promoter::GFP fragment to detect by PCR, but not enough to detect fluorescence. Obtaining multiple independent segregants for each microinjection, or performing each injection at least twice, would help avoid complications with copy number and could validate expression patterns or loss of GFP fluorescence.

Since complete loss of GFP expression is seen from the *ZK829.4*$_{\text{promoter(-445)}}$::GFP to the *ZK829.4*$_{\text{promoter(-414)}}$::GFP construct, the region of sequence between -445bp and -414bp was analyzed for predicted transcription factor binding sites. Pairwise alignment of the promoter regions (-1167bp to +50bp) of *C. elegans ZK829.4* and its ortholog in *C. briggsae* showed two sections of perfectly conserved sequence in this area (Figure 5). The sequence between -452bp and -391bp was inputted into TESS for analysis. The top three hits returned were for STE12, GATA-1, and Sp1 (specificity protein 1) (Figure 5, Table 3). Sequences from *C. brenneri* and *C. remanei* were not used for comparison since they are sexually reproducing species. Due to the sexual nature of *C. brenneri* and *C. remanei*, these species need to be highly inbred to establish homogeneity within the

population. Since whole-genome shotgun sequencing requires overlap between individual reads, allelic heterozygosity may confound sequence assembly and lead to complications during comparative genomic analyses (Barriere et al. 2009). Consequently, only the selfing hermaphroditic strains, *C. elegans* and *C. briggsae*, were used for promoter sequence comparison.

STE12 is transcription factor in yeast that regulates the expression of genes required for mating, as well as genes involved in filamentation under conditions of nutrient deprivation (Elion et al. 1993; Liu et al. 1993). Since I was unable to find a homolog for STE12 outside of Saccharomycetaceae, no further consideration was given to STE12 as a possible transcription factor for *C. elegans* GDH.

GATA-1 plays an important role in erythroid development, and is expressed in hematopoietic cell lineages (Yamamoto et al. 1997). In *C. elegans*, *end-1* encodes a GATA-like transcription factor that functions in endoderm development (Zhu et al. 1997). Since nutrient processing and metabolism occurs in the gut, it is possible that GDH activity needs to be expressed at greater levels in this tissue type, and that the boost in expression is driven by *end-1*.

Sp1 binds to GC box elements (`5′-(G/T)GGGCGG(G/A)(G/A)(C/T)-3′`) and is involved in the early development of an organism. Recent studies have also indicated a role for Sp1 in the regulation of genes in response to insulin, such as the insulin receptor (IR) (Solomon et al. 2008). Since GDH activity contributes to insulin release by pancreatic β-cells, it is possible that activation of Sp1 could represent a positive feedback mechanism for insulin signalling if it upregulates expression of GDH. Alternatively, it is possible that this region of the *let-56* promoter contains a novel transcription factor

binding site specific to *Caenorhabditis*, since the level of conservation between *C. elegans* and *C. briggsae* is so high in the area.

In this section of the thesis I found a 31bp window containing a putative *cis*-regulatory element responsible for GDH expression by performing a promoter::GFP cut down analysis. Investigation of the sequence led to the identification of three possible TFs that may regulate *ZK829.4*: STE12, GATA-1, and Sp1. Further work needs to be done to refine the promoter region and define the exact sequence necessary for driving expression of GDH.

CHAPTER 3: DETERMINATION OF THE IMPORTANCE OF THE 3' UTR IN REGULATION OF *LET-56* EXPRESSION

3.1 Introduction

microRNAs (miRNAs) are small, non-coding RNAs that have sequences complementary to coding regions of messenger RNAs (mRNAs). Via their complementarity, miRNAs block expression by inhibiting translation or targeting the mRNA for degradation. Multiple miRNA binding sites have been predicted for the 3' UTR of *ZK829.4*, by the computational prediction programs miRanda and PicTar (Figure 7). miRanda has also predicted multiple miRNA binding sites to exist in the 3' UTR of the human ortholog, GLUD1 (Betel et al. 2008). miRanda predictions are based on sequence complementarity of the mRNA target site to known miRNAs, with the seed region of the miRNA being given higher consideration. The seed region is the first 7 or 8 nucleotides of the miRNA (the 5' end), which has been observed to display greater evolutionary conservation than the 3' end (Lim et al. 2003). miRanda also takes into consideration the stability of the RNA-RNA duplex, as well as the level of conservation of the mRNA target site across related genomes (Martin et al. 2007). PicTar searches for multiple binding sites in a 3' UTR using sets of coexpressed miRNAs, and is biased towards perfect complementarity of the seed region. It also requires conservation of the

Figure 7. Predicted miRNA binding sites in the *let-56* 3' UTR

miRanda and PicTar predict multiple miRNA binding sites for the 3' UTR of *ZK829.4*. There are two alternative transcripts of the 3' UTR, one whole (*ZK829.4.1* and *ZK829.4.3*) and one spliced (*ZK829.4.2*). Splicing creates three miRNA binding sites (mir-239b, mir-239a, and mir-244) while eliminating 13 others. (Figure modified from WormBase, WS190)

mRNA target site across several species (Lall et al. 2006; Martin et al. 2007). Here, I investigate the validity of the predicted miRNA binding sites.

To experimentally test the predicted miRNA targets I looked broadly at the importance of the let-56 3' UTR in regulating expression levels of GFP by generating chimeric GFP reporter constructs. The *ZK829.4* promoter region (~1100bp) was fused to GFP, and then fused to the *unc-54* 3' UTR as a control, or to variants of the *ZK829.4* 3' UTR. The *unc-54* 3' UTR acts as an mRNA stabilizer, and is commonly used for promoter::GFP fusions in *C. elegans*. There are two transcripts of the *ZK829.4* 3' UTR, one unspliced (*ZK829.4.1* and *ZK829.4.3*) and one spliced (*ZK829.4.2*). The spliced form generates three new miRNA binding sites (mir-239b, mir-239a, and mir-244), while eliminating 13 others (Figure 8). Two independent ESTs, *yk1504d06.3* and *yk1407e05.3*, validate the existence of the spliced 3' UTR transcript. It is possible that these two transcripts are differentially expressed or regulated within *C. elegans*. Therefore three different variants of the *ZK829.4* 3' UTR were examined: 1. the whole 327bp, 2. the spliced transcript, and 3. the last 154bp of the spliced transcript, excluding the 8bp prior to the intron and effectively eliminating the three new miRNA binding sites formed after splicing (Figure 8). I refer to the first construct as "*ZK829.4* 3' UTR_{whole}", the second construct as "*ZK829.4* 3' $UTR_{spliced}$", and the third construct as "*ZK829.4* 3' $UTR_{variant}$".

In this section, I generate chimeric GFP reporter constructs containing the different 3' UTRs to assess the regulatory role of the miRNA binding sites in the *ZK829.4* 3'UTR. I determine that the level of expression and the number of tissues with expression inversely correlate with how many miRNA binding sites are available. I also analyze the relative levels of expression of the two 3' UTR transcripts in each of the

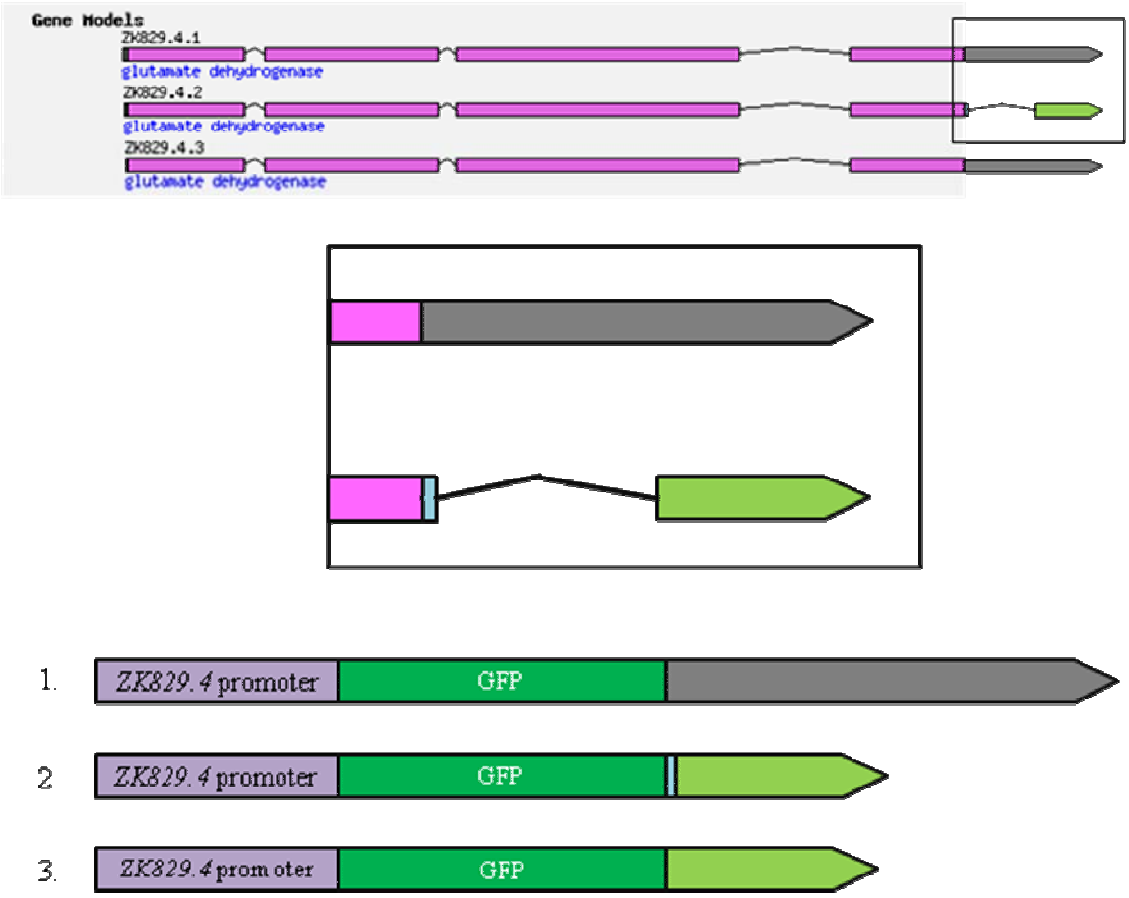

Figure 8. ZK829.4 3' UTR chimeric constructs

Three different *ZK829.4* 3' UTR variants were analyzed using chimeric GFP reporter constructs to determine the differential regulation exerted by the generation or removal of miRNAs after splicing. The first construct contains the whole 3' UTR (*ZK829.4* 3' UTR_{whole}), the second contains the spliced 3' UTR (*ZK829.4* 3' $UTR_{spliced}$), and the third contains the last 154bp of the spliced 3' UTR, excluding the first 8bp (*ZK829.4* 3' $UTR_{variant}$). (Note: the figure is not to scale)

developmental stages of *C. elegans* by quantitative real-time PCR (qRT-PCR), to assess whether there are alternative requirements for the two transcripts during development.

3.2 Materials and Methods

3.2.1 Total RNA extraction

Total RNA was extracted from each sample with the aid of Nihar Bhattacharyya according to ShuYi Chua's total RNA isolation protocol. N2 nematodes were grown to gravid adulthood and were bleached with a 2.4% sodium hypochlorite (Bioshop Cat: SYP001.1), 0.5N NaOH (Fisher Scientific Cat: S-318B) solution to fragment worm bodies and release fertilized eggs. Isolated eggs were hatched in M9 overnight on a platform mixer. Under these starved conditions, *C. elegans* L1s arrest as early L1 larvae. These newly hatched nematodes were collected to obtain the L1-starved (L1-s) sample. To obtain the other stages, L1-s nematodes were plated onto OP50 seeded plates and incubated at 20˚C. Fed L1s were collected after 7 hours, L2s after 23hours, L3s after 29 hours, L4s after 46 hours, and young adults (prior to egg lay) after 51 hours on OP50. RNA was extracted from each sample using Trizol (Invitrogen Cat: 15596-026) and chloroform (Caledon Cat: 3000-3) successively, then precipitated using 2-propanol (Caledon Cat: 8601-2). The RNA pellet was washed with 0.5mL 75% ethanol, allowed to air-dry, and resuspended in 0.1% v/v DEPC-treated (Sigma Cat: D5758) ddH_2O. Concentration readings were taken using a Nanodrop (ND-1000) spectrophotometer, and 50ng was visualized on a 1% agarose (Bioshop Cat: AGA001) gel to determine RNA quality before proceeding. RNA samples were then treated with DNase I (Invitrogen Cat: 18068-015), and subsequently purified following the RNA Cleanup protocol in the QIAgen RNeasy® Mini Kit (Cat: 74104).

3.2.2 Generation of cDNA samples

cDNA samples were generated by Nihar Bhattacharyya following the Fermentas RevertAid^{TM} H Minus First Strand cDNA Synthesis Kit (Fermentas Cat: K1632) protocol, using an oligo$(dT)_{17}$ primer. 250ng of total RNA was used to generate each cDNA sample.

3.2.3 Quantitative RT-PCR

Quantitative RT-PCR was run using the iQ^{TM}5 Multicolor Real-Time PCR Detection System (Bio-Rad) with the aid of Jeff S. Chu and Nihar Bhattacharyya. Sequences for *let-56* and *rpl-19* were obtained from WormBase (WS197). *rpl-19*, which encodes large ribosomal subunit L19 protein, was used as a control since it is expressed at roughly equivalent levels throughout the life cycle of *C. elegans*. Primers used for *rpl-19* were: rpl19-F: `GAGAA CAAGA GAGCC AAGCA A`, and rpl19-R: `CTTGA CGACT TGTCT CTCCT CA` (product size: 99bp). Primers used to detect the whole *ZK829.4* 3'UTR were: qRTwhole-F: `CTCTG ATCTT TTCTG CCTGG T`, and qRTwhole-R: `GTCCC GAACC AACAA ACAAC` (product size: 114bp). Primers used to detect the spliced *ZK829.4* 3'UTR transcript were: qRTspliced-F: `GTACA ACCTT GGACT TGATA`, and qRTspliced-R: `AAAGT GAGAA GTGGG TACTT`, which spans either side of the splice junction (product size: 115bp) (Figure 9). All samples were run in triplicate using the iQ^{TM} SYBR® Green Supermix (Bio-Rad Cat: 170-8880). The program run was "2step+melt", which has 35 cycles of 10-second melts at 95˚C and 30-second elongations at 60˚C, followed by a melting curve of 36 10-second cycles from 60˚C to 95˚C (increasing by 1˚ each cycle). Outliers from the triplicate runs were removed, and results were normalized to *rpl-19* levels of expression.

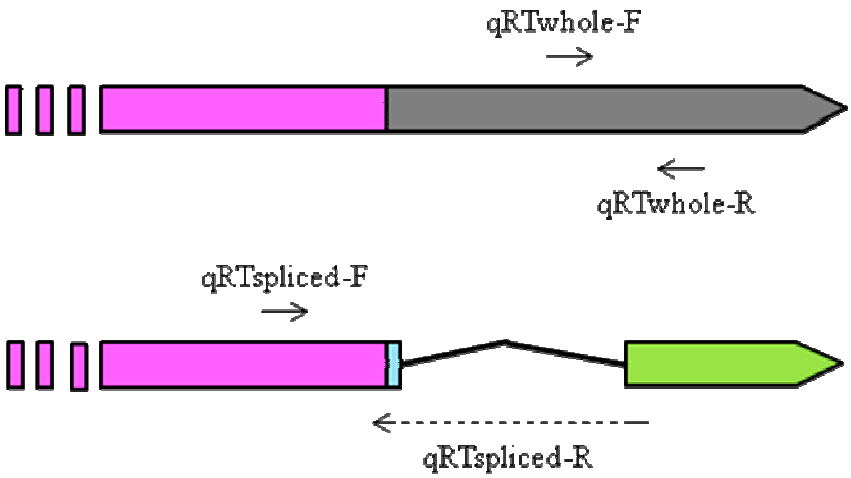

Figure 9. Location of primers used to detect the two ZK829.4 3' UTR transcripts by qRT-PCR

Location of the sets of primers used to identify expression levels of the two endogenous transcripts of the *ZK829.4* 3' UTR by qRT-PCR. □□□ indicates gene continues in the 5' direction. Figures are not to scale.

3.2.4 Generation of *ZK829.4*$_{promoter}$::GFP::3' UTR chimeric constructs

To determine the importance of the *ZK829.4* 3' UTR in regulating gene expression, chimeric GFP reporter constructs were generated containing the endogenous *ZK829.4* promoter region fused to GFP, and fused to either the *unc-54* 3' UTR as a control, or variants of the *ZK829.4* 3' UTR. Phusion polymerase was used for all PCRs to ensure fidelity. The *pPD95.67 (GFP)* coding cassette was used to amplify GFP and *unc-54* 3' UTR sequences. N2 genomic DNA was used to amplify the *ZK829.4* promoter and 3' UTR regions. Sequences for the *ZK829.4* promoter and 3' UTR were obtained from WormBase (WS184).

a. *ZK829.4*$_{promoter}$::GFP::*unc-54* 3' UTR chimeric construct

The *ZK829.4* promoter (-1100bp) was amplified off of N2 genomic DNA using primers including restriction sites for HindIII (forward) and PstI (reverse): prom-A*: CGGC**A AGCTT** CAAGC TCACG TTTTA TCATT CTTG, and prom-B*: TTGC**C TGCAG** GAAAG AGTGC TCAAC ATTAC CTGA. Amplified promoter and *pPD95.67* were both double-digested with HindIII (Fermentas FastDigest^{TM} Cat: ER0504) and PstI (Fermentas FastDigest^{TM} Cat: ER0614). The *pPD95.67* vector was subsequently dephosphorylated with alkaline phosphatase (AP) (Roche Cat: 713 023). Digested products were PCR purified (QIAgen Cat: 28106) and then ligated overnight with T4 DNA ligase (New England Biolabs Cat: M0202S). 5µL of the ligation reaction was used to transform competent DH5α cells (see 2.2.3 DH5α transformation). Individual colonies were inoculated in LB media containing ampicillin (amp) (Sigma Cat: 271861-5G), grown overnight and miniprepped (QIAgen Cat: 27106). Purified plasmid was then restriction

digested with NdeI (New England Biolabs Cat: R0111S) to ensure the construct was the correct size (three bands: 595bp, 957bp, and 3975bp).

b. *ZK829.4*$_{promoter}$::GFP::*ZK829.4* 3' UTR variant constructs

The *ZK829.4* 3' UTR regions were amplified off of N2 genomic DNA. Forward and reverse primers had an EcoRI digestion site or an ApaI digestion site added on, respectively. The reverse primer used to amplify all three *ZK829.4* 3' UTR variants was: 3'UTR-B*: TTGC**G GGCCC** AATGA CCATG TAGAA GTGTT TAAGG. The forward primer used to amplify *ZK829.4* 3' UTR$_{whole}$ was: 3'UTRwhole-A*: CAGC**G AATTC** GTACC CACTT CTCAC TCATC TCA. The forward primer used to amplify the *ZK829.4* 3' UTR$_{spliced}$ was: 3'UTRspliced-A*: CAGC**G AATTC** GTACC CACTT CTCAC TTTAG TATAA TTAAA TATT. The forward primer used to amplify *ZK829.4* 3' UTR$_{variant}$ was: 3'UTRvariant-A*: CAGC**G AATTC** TTCTC ACTTT AGTAT AATTA AATAT T. Following PCR amplification, the 3' UTR construct and *pPD95.67* were double-digested with EcoRI (Fermentas FastDigest^{TM} Cat: FD0274) and ApaI (Fermentas FastDigest^{TM} Cat: ER1414). Digestion of *pPD95.67* with EcoRI and ApaI excises the *unc-54* 3' UTR. Following digestion, the *pPD95.67* vector was dephosphorylated. Both vector and 3' UTR were PCR purified and then ligated overnight using T4 DNA ligase. 5µL of the ligation reaction was used to transform DH5α competent cells. Individual colonies from successful transformants were inoculated in LB AMP media overnight. Cultures were then miniprepped. The plasmid was then digested with NdeI to ensure correct plasmid size (two bands: 1148bp and 2864bp). The GFP::*ZK829.4* 3' UTR construct was then double-digested with HindIII and PstI, dephosphorylated with AP, and PCR purified before being ligated to the *ZK829.4* promoter. Competent DH5α cells were transformed

with 5μL of the ligation reaction, and successful colonies grown overnight in LB AMP media. The cultures were then miniprepped, and digested with NdeI to ensure the correct plasmid was purified.

3.2.5 Generating competent DH5α cells

DH5α cells were made competent using $CaCl_2$ according to a protocol developed by Keith A. Boroevich. A 5mL culture of DH5α cells in LB media were grown overnight in the 37˚C shaker. 1mL of culture was added to 100mL of fresh LB media and incubated for 4 hours at 37˚C until A_{600} was 0.420, indicating that the cells were in log phase. The culture was then incubated on ice for 20 minutes before being spun down at 5000rpm for 3 minutes. The supernatant was decanted, and the pellet resuspended in 10mL of 100mM $CaCl_2$ and incubated on ice for 1 hour. The cells were again spun down at 5000rpm for 3 minutes and the supernatant decanted. The pellet was resuspended in 5mL of 100mM $CaCl_2$ and incubated on ice for another 1 hour. Cells were now competent, and were stored in 200μL aliquots (20% glycerol) at -80˚C.

3.2.6 DH5α transformation

Transformations of DH5α were performed according to a protocol developed by Keith A. Boroevich. 200μL of competent DH5α cells were used for each transformation. Cells were first thawed on ice. Plasmid was added to the cells, mixed gently, and then incubated on ice for 10 minutes. Cells were then heat-shocked at 42˚C for 45 seconds, and then incubated on ice for another 10 minutes. 800μL of fresh LB media was added to the cells, and they were incubated at 37˚C for 1 hour. The culture was spun down at 3000rpm for 1 minute and 800μL of the supernatant was removed. Cells were

resuspended in the remaining 200µL, and 50µL was plated onto LB agar containing ampicillin. Plates were incubated at 37˚C overnight.

3.2.7 Microinjection

See section 1.2.6 Microinjection for a complete description of microinjection. All injections were done by Domena K. Tu. *ZK829.4*$_{\text{promoter}}$::GFP::3' UTR chimeric constructs were coinjected with *pCeh361* at final concentrations of 20ng/µL and 100ng/ µL, respectively. Refer to Appendix G for a complete list of strains generated in this section.

3.2.8 Transgene integration into the genome

P_0 worms from BC8180; sEX1902 (*dpy-5(e907)/dpy-5(e907) [ZK829.4*$_{promoter(-1100)}$*::GFP::ZK829.4 3'UTR*$_{whole}$*+pCeh361]*) and BC8181; sEX1903 (*dpy-5(e907)/dpy-5(e907) [ZK829.4*$_{promoter(-1100)}$*::GFP::unc-54 3'UTR+pCeh361]*) were treated with 1,500R of X-ray irradiation (Torex 150D X-ray Inspection System, settings: 145kV @ 5mA on shelf 7 for 135 seconds) to create stable GFP-expressing lines. P_0s were allowed to recover for one hour at 20°C before young adult hermaphrodites were individually plated onto 100 x 15mm Petri plates seeded with OP50, and incubated at 23°C for 5 days. Wildtype (*dpy-5* rescued) F_2 progeny were then plated individually, and the F_3 generation was scored for lines producing 100% rescued *dpy-5* progeny. Irradiated stable lines were backcrossed to the wildtype N2 strain three times to eliminate background mutations.

3.2.9 Microscopy

See section 1.2.10 Materials and methods for a detailed description on microscopy. GFP expression pattern analysis was done using a Zeiss Axioscope equipped

with a QImaging camera and a GFP filter. All GFP images were taken under identical filter, lens, and camera settings. Exposure times are indicated on the figures. Only strains expressing GFP were imaged.

3.3 Results

3.3.1 Quantitative RT-PCR

To evaluate the differences in expression levels of the *ZK829.4* 3' UTR transcripts across each developmental stage of *C. elegans*, qRT-PCR was conducted using transcript-specific primers against cDNA samples from each stage (Figure 9). Results were analyzed using the ΔC_T Method Using a Reference Gene (http://www.bio-rad.com), which is a variation of the Livak method commonly used to evaluate normalized expression (Livak and Schmittgen 2001; Schmittgen and Livak 2008). The ΔC_T Method Using a Reference Gene uses the difference between sample and reference C_T values to determine differences in expression levels between samples (refer to Appendix H for a complete table of results and a sample calculation). Single outliers for the L3 3' UTR_{whole} sample and for the L2 3' UTR_{whole} sample were removed. Results were normalized to the expression levels of *rpl-19*, which was run as an endogenous internal standard. *rpl-19* encodes a large ribosomal subunit L19 protein that is expressed at a fairly constant level throughout development, and is commonly used as a standard for qRT-PCR. I found that *ZK829.4* 3' $UTR_{spliced}$ is consistently expressed at a greater level than *ZK829.4* 3' UTR_{whole} at each developmental stage (Figure 10). Expression levels are greatest in the L1-s stage, with all other stages being roughly equivalent.

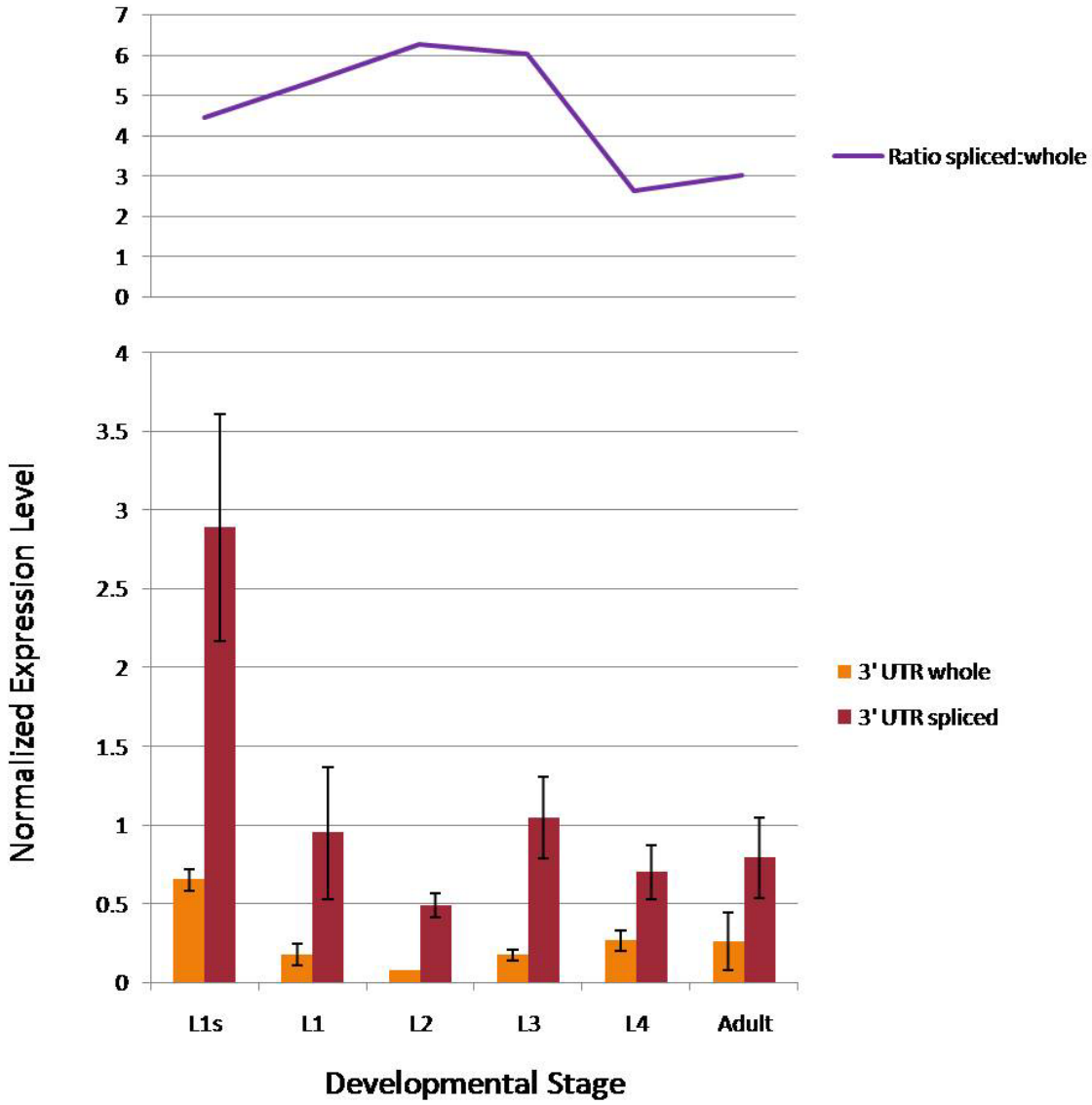

Figure 10. qRT-PCR analysis of the two ZK829.4 3' UTR transcripts

ZK829.4 3' $UTR_{spliced}$ is consistently expressed at a greater level than the unspliced form, at each of the developmental stages. The overall level of expression is much greater at the L1-starved stage, with the rest of the stages having roughly similar levels. Comparison of the spliced 3' UTR expression levels with the whole 3' UTR expression levels shows a peak in expression of the spliced 3' UTR transcript at the L2 stage. Results were normalized to expression levels of *rpl-19*, which encodes a large ribosomal subunit protein. Refer to Appendix H for the raw qRT-PCR data, and a sample calculation for obtaining normalized expression levels.

3.3.2 Chimeric GFP reporter constructs

To examine the importance of the *ZK829.4* 3' UTR in regulating expression of GDH, I generated chimeric GFP reporter constructs containing the endogenous *ZK829.4* promoter fused to GFP, and fused to different 3' UTRs. The *unc-54* 3' UTR was used as a control, since it is used for most promoter::GFP transgene constructs in *C. elegans*. I also tested the whole *ZK829.4* 3' UTR, the spliced transcript, and the last 154bp of the spliced variant, excluding the first 8bp that helps form three new miRNA binding sites (Figure 8). Of the four reporter cassettes, the transgenic organisms containing the *unc-54* 3' UTR (BC8181; sEX1903) displayed the highest levels of GFP expression, which is expected since it acts as an mRNA stabilizer. For the *ZK829.4* 3' UTR variations, level of GFP expression was inversely related to the number of miRNA binding sites available on the 3' UTR. The highest level of expression was seen in transgenic nematodes containing the *ZK829.4* 3' $UTR_{variant}$ (BC8525; sEX2220), followed by *ZK829.4* 3' $UTR_{spliced}$ (BC8519; sEX2215), and lastly *ZK829.4* 3' UTR_{whole} (BC8180; sEX1902) (Figure11). The expression patterns also differ between the four constructs, with the *unc-54* 3' UTR and *ZK829.4* 3' $UTR_{variant}$ having expression in the greatest number of tissues, followed by *ZK829.4* 3' $UTR_{spliced}$, and *ZK829.4* 3' UTR_{whole} (Table 4).

Somatic mosaic loss of extrachromosomal DNA arrays is commonly observed in *C. elegans* transgenics, resulting in patchy and inconsistent expression patterns (Herman 1984). Consequently, I integrated the *ZK829.4*$_{promoter}$::GFP::*unc-54* 3' UTR and the *ZK829.4*$_{promoter}$::GFP::*ZK829.4* 3' UTR_{whole} transgenes into the genome via treatment with X-ray irradiation. Since X- irradiation can result in multiple mutations besides transgene integration, I outcrossed the integrated strains thrice with the wildtype N2 strain. I

Table 4. Expression patterns of the different ZK829.4promoter::GFP::3' UTR constructs

	Chimeric GFP reporter constructs			
Tissue	***unc-54* 3' UTR**	**3' $UTR_{variant}$**	**3' $UTR_{spliced}$**	**3' UTR_{whole}**
Pharyngeal bulbs	+	+	+	+
Pharynx	+	+	+	+
Gut	+	+	+	
Hypoderm	+	+	+	
Muscle	+	+		
Anterior neurons	+	+		

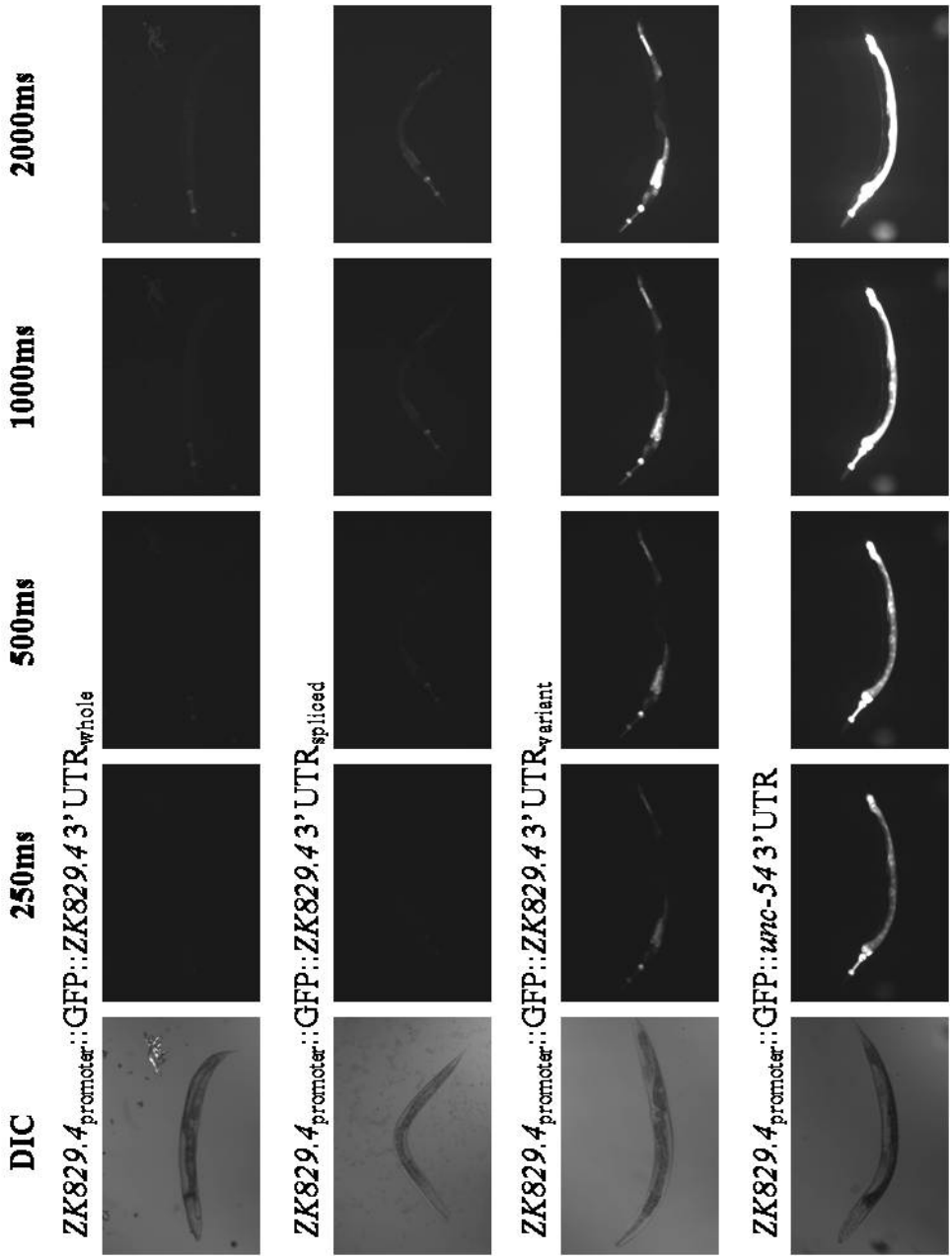

Figure 11. Expression patterns of the *ZK829.4*$_{promoter}$::GFP:: 3' UTR constructs

Expression patterns driven by the various *ZK829.4*$_{promoter}$::GFP::3' UTR constructs in the non-integrated strains. All nematodes imaged were young adults to ensure roughly equivalent levels of expression. GFP expression was greatest with the *unc-54* 3' UTR construct, and least with the *ZK829.4* 3' UTR$_{whole}$ construct.

retained a cleaned GFP/GFP line for the *unc-54* 3' UTR strain (BC8565; sIS1903). Since the GFP expression for the *ZK829.4* 3' UTR_{whole} transgene was too low to follow via microscopy, I attempted to follow GFP via PCR using GFP-specific primers. Although I successfully outcrossed the strain, I was unable to find and maintain a homozygotic GFP-containing line. The expression patterns for the integrated strains are similar to their non-integrated counterparts, although intensities slightly decreased (Figure 12). Due to time constraints, I was unable to integrate the strains containing the *ZK829.4* 3' $UTR_{spliced}$ and *ZK829.4* 3' $UTR_{variant}$ transgene constructs.

3.4 Discussion

Numerous miRNA binding sites have been predicted for the 3' UTR of *ZK829.4* by the computational programs miRanda and PicTar, however whether the 3' UTR exerts regulatory control over expression of GDH has not been validated. Two transcripts of the 3' UTR exist, one spliced and one unspliced, that differ in the number of miRNA binding sites indicating that they may be differentially regulated and expressed, spatially and/or temporally (Figure 7). Through qRT-PCR analysis, I determined that the *ZK829.4* 3' $UTR_{spliced}$ transcript is always expressed at a higher level (3- to 6-fold) than the *ZK829.4* 3'UTR_{whole} transcript, correlating well with the GFP data (Figure 10, 11). The higher expression level seen in the L1-s stage is in accord with the function of GDH in producing α-ketoglutarate. During times of starvation, when the mitochondria are low in energy, it would be necessary to shunt α-ketoglutarate through the Krebs cycle to increase energy production. Alternatively, when food is available, it may not be necessary for GDH production of α-ketoglutarate at such high levels, resulting in the decreased GDH expression seen in the other developmental stages (Figure 10). In

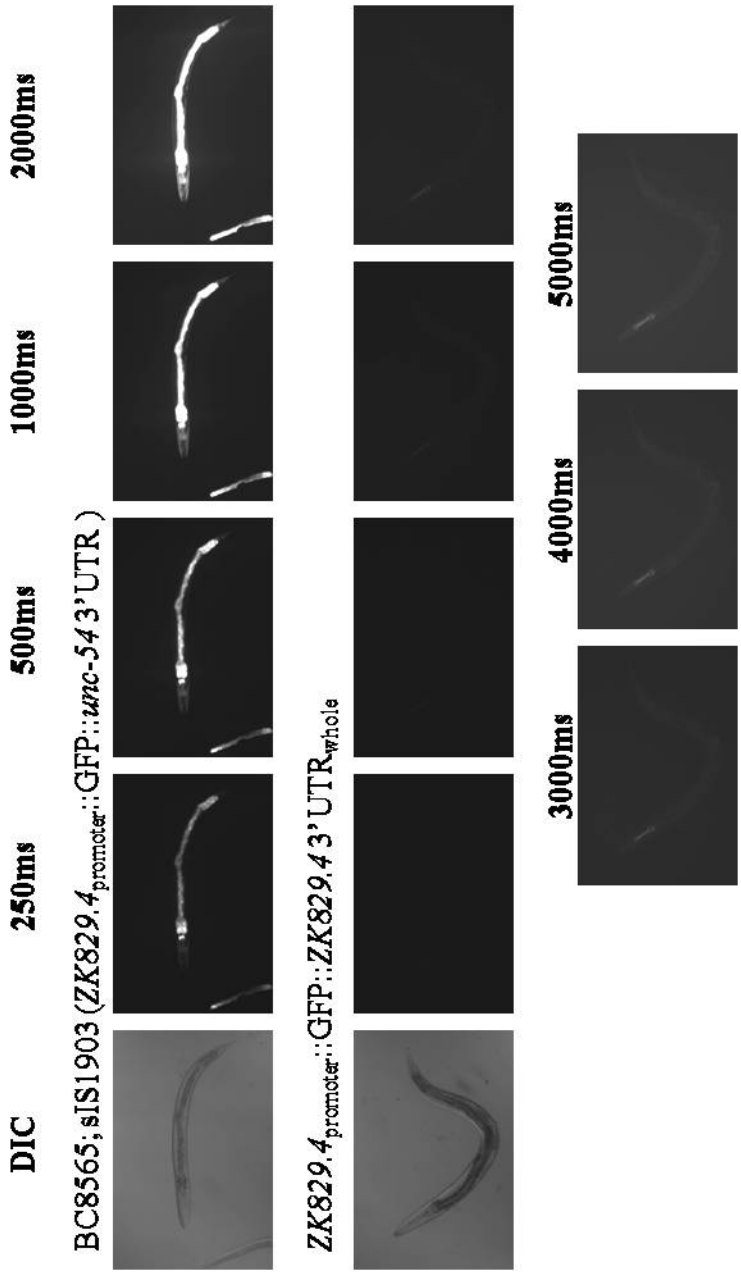

Figure 12. Expression patterns of integrated *ZK829.4*$_{promoter}$::GFP::3' UTR strains

The *ZK829.4*$_{promoter}$::GFP::*unc-54* 3' UTR and *ZK829.4*$_{promoter}$::GFP::*ZK829.4* 3' UTR$_{whole}$ transgenes were integrated by treatment with 1500rads of X-ray to eliminate random somatic loss. The resultant nematodes had similar expression patterns to the original transgenics. Only the strain containing the *unc-54* 3' UTR was successfully outcrossed.

addition, a peak in expression of the spliced 3' UTR transcript compared to the whole 3' UTR transcript was seen at the L2 stage (Figure 10), indicating a possible role for the 3' UTR in mediating temporal regulation of GDH expression.

Through the creation and screening of GFP reporter gene constructs driven by the endogenous *ZK829.4* promoter and differing in the attached 3' UTR, I have determined that the *ZK829.4* 3' UTR plays a role in regulating the level and spatial pattern of GDH expression. When the *unc-54* 3' UTR or the *ZK829.4* 3' $UTR_{variant}$ construct were used, GFP expression was high, being easily seen at 100ms and 250ms, respectively. However, both the *ZK829.4* 3' UTR_{whole} and *ZK829.4* 3' $UTR_{spliced}$ constructs had significantly lower expression, not being seen until 2000ms and 1000ms, respectively (Figure 11). These results suggest that the miRNA binding sites in the 3' UTR help downregulate expression of the *ZK829.4* mRNA transcript. In addition, *ZK829.4* 3' $UTR_{variant}$ had GFP expression in the greatest number of tissues, and *ZK829.4* 3' UTR_{whole} in the least number of tissues (Table 4). This indicates that the miRNA binding sites in the 3' UTR of *ZK829.4* may also help regulate tissue-specific expression of GDH, since both the *unc-54* 3' UTR and the *ZK829.4* 3' $UTR_{variant}$ constructs displayed expression in additional tissues compared to the transgenes containing the endogenous transcripts of the *ZK7829.4* 3' UTR. However, since GFP expression is so low in transgenic organisms containing the *ZK829.4* 3' UTR_{whole} chimeric construct, it is also possible that both *ZK829.4* 3' UTR_{whole} and *ZK829.4* 3' $UTR_{spliced}$ have similar expression patterns, if GFP in the gut and hypoderm simply cannot be detected over background fluorescence (Figure 11).

Here it is also interesting to note that the 3' UTR of the current *ZK829.4* gene model can also be extended based on the predicted miRNA binding sites, since mir-237

and mir-62 lie outside of the annotated 3' UTR region (Figure 7). Confirmation of 3' UTR extension could be done by sequencing the 3' end of *ZK829.4* from cDNA samples.

In this section of the thesis, I conclude that the *ZK829.4* 3' UTR does play a role in downregulating expression of GDH. Further work needs to be done to validate the regulatory role of individual putative miRNA binding sites in the 3' UTR. I also determine that the spliced 3' UTR transcript has a greater expression level that the unspliced variant, which is reflected in both the qRT-PCR data, and the chimeric GFP reporter constructs (Figure 10, 11). Since *ZK829.4* 3' $UTR_{spliced}$ has fewer miRNA binding sites than *ZK829.4* 3' UTR_{whole}, these results provide further evidence for the authentication of the miRanda and PicTar miRNA predictions. Differences in the GFP expression patterns mediated by the 3' UTR transcripts, and spliced:whole 3' UTR expression ratios, indicate a plausible role for the 3' UTR in directing spatiotemporal regulation of GDH (Figure 11). Since somatic mosaic loss of exogenous DNA can occur in transgenic strains, as mentioned previously, reinjection of the chimeric GFP::3' UTR reporter constructs could be done to confirm the observed differences in expression patterns for the spliced and unspliced *ZK829.4* 3' UTRs.

CHAPTER 4: THE IMPORTANCE OF THE GTP-BINDING SITE IN REGULATING GDH ACTIVITY IN C. ELEGANS

4.1 Introduction

Glutamate dehydrogenase functions as a homohexamer to catalyze the reversible oxidative deamination of glutamate to α-ketoglutarate and ammonia. Located in the inner mitochondrial matrix, GDH activity feeds the TCA cycle to increase the production of energy. GDH is tightly regulated within the cell since its function is closely tied to energy levels, and also to amino acid catabolism. Correspondingly, GDH is allosterically negatively affected by GTP, and allosterically positively affected by ADP and leucine (Sener and Malaisse 1980; Dieter et al. 1981). These interactions indicate that GDH is inhibited when mitochondria are rich in triphosphates, and activated when mitochondria are low in energy, or when catabolism of amino acids is high. Interestingly, mutations in the GTP binding site of human GDH result in a dominant hyperinsulinism and hyperammonemia (HI/HA) phenotype (Stanley et al. 1998). These mutations are dominant since mature GDH functions as a homohexamer, and presumably, each protein on average will consist of half wildtype and half mutant monomers. Stanley et al. (1998) propose that increased GDH activity due to loss of negative allosteric inhibition results in a rise of the cellular ATP to ADP ratio as α-ketoglutarate is fed into the Krebs cycle. This change in the phosphate potential causes the ATP-sensitive potassium (K_{ATP}) channels to open, depolarizing the membrane and opening the voltage-gated Ca^{2+} channels. The

increase in cytoplasmic Ca^{2+} levels in the pancreatic beta cells then triggers the release of insulin stored in secretory vesicles, resulting in the hyperinsulinism phenotype. Hyperammonemia could result directly from GDH overactivity due to increased oxidation of glutamate to produce ammonia. In addition, it has been proposed that lower concentrations of glutamate could impair urea synthesis by carbamoylphophate synthetase (CPS) in the liver, since glutamate is a precursor of N-acetyl-glutamate, which is necessary for activation of CPS (Stanley et al. 1998).

In this section of the thesis, I examine whether *C. elegans* glutamate dehydrogenase exerts similar regulatory control over insulin levels in the nematode, and whether this insulin regulation is similarly affected by mutations in the GTP-binding site. I do this by generating a GDH transgene with a mutation commonly found in individuals with HI/HA and injecting it directly into the nematode. Since mutations preventing allosteric inhibition by GTP are dominant (Stanley et al. 1998), I expect the mutant transgene to also act in a dominant manner within *C. elegans*. On recommendation by Marco Gallo (Riddle Lab, UBC), the GTP-mutant construct (*ZK829.4(G477D)*) was injected directly into a stable DAF-28::GFP strain (VB1605; svIS69), generously provided by Simon Tuck (Kao et al. 2007) with the aid of Marco Gallo. *daf-28* encodes a beta-type insulin homologous to human insulin, and is expressed in the ASI and ASJ neurons of the head, which function in dauer formation, chemotaxis, navigation (ASI), and lifespan (ASJ) (Li et al. 2003). From this analysis, I determine that *C. elegans* GDH exhibits similar control over insulin secretion, and that it is negatively regulated by GTP.

4.2 Materials and Methods

4.2.1 Construction of the GDH transgene with a GTP-binding site mutantion

The fosmid *WRM069dG08* was digested with XbaI (Fermentas FastDigest™ Cat: ER0684), and the 5412bp band contained the entire *let-56* gene (including 1155bp of the promoter sequence and the entire 3' UTR) gel extracted (QIAgen Cat: 28704). *pBluescript* was also digested with XbaI and dephosphorylated with AP. *let-56* was ligated to *pBluescript* using T4 DNA ligase, and the ligation used to transform competent DH5α cells. Successful transformants were distinguished via blue-white selection using LB AMP plates with X-gal (Invitrogen Cat: 15520-018) and IPTG (Invitrogen Cat: 15529-019). Individual colonies were grown in LB AMP media overnight at 37˚C and miniprepped the next day. The plasmid was then mutated using DpnI site-directed mutagenesis according to Carrie L. Simms' protocol. DpnI digests methylated DNA. The *let-56::pBluescript* construct was first single-strand PCR amplified using a mutant primer targeting the GTP-binding site: GTP-F: CGATG TCTTT CTCGG AAGC**A T**CAGC GATCT TG. This site was chosen based on the results of Stanley et al. (1998), when they sequenced 8 patients with HI/HA (Figure 13). The most common mutation (G446D) was chosen to mimic. The PCR product was treated with DpnI (New England Biolabs Cat: R0176S) for 1 hour at 37˚C to digest the original miniprepped plasmid. 5μL of the resulting single-stranded mutant plasmid DNA was then used to transform competent DH5α cells. Successful transformants were cultured in LB AMP media overnight at 37˚C and miniprepped. Isolated plasmid was digested with XbaI to ensure correct size (two bands: 2961bp and 5412bp) before sending to Macrogen Korea for sequencing to check for the GTP-binding site mutation (*ZK829.4(G477D))*.

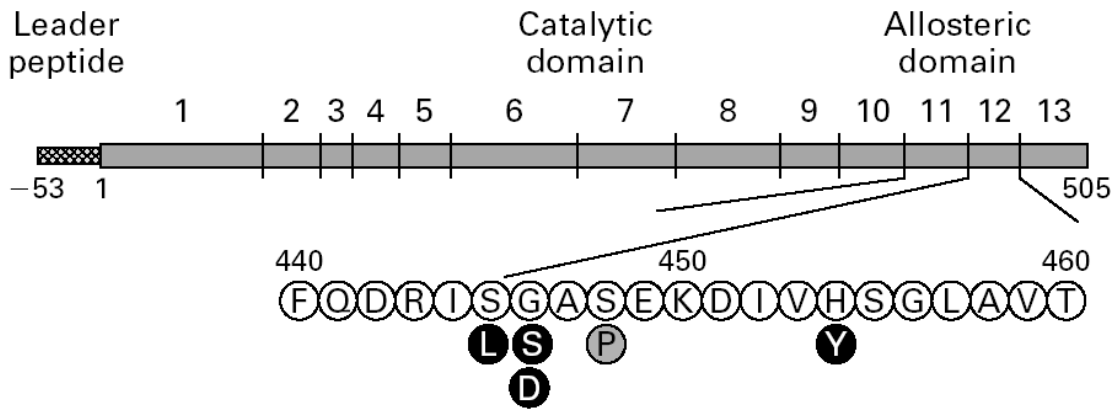

Figure 13. GDH mutations found in individuals with HI/HA (Stanley, Lieu, et al., 1998)

Stanley et al. (1998) sequenced the GDH gene in eight cDNA samples generated from patients exhibiting the HI/HA syndrome. The most commonly mutated residue was glycine 446, with two cases of G→D, and one of G→S. In addition, two individuals displayed the S445L mutation, another two individuals displayed the S448P mutation, and one individual had the H454Y mutation. Those patients with the S448P mutation displayed clinically milder symptoms (grey) than the others (black). (Figure obtained from Stanley et al., 1998)

4.2.2 Microinjection

See section 1.2.6 Materials and methods for a complete description of microinjection. All injections were done by Domena K. Tu. The *ZK829.4(G477D)* construct was injected at a final concentration of 25ng/µL alongside *pCFJ104* at 5ng/µL and *pCeh361* at 100ng/µL. The *pCFJ104* plasmid drives mCherry expression in the muscle, driven by the *myo-3* promoter (*myo-3*$_{promoter}$::GFP::*unc-54* 3' UTR). *ZK829.4(G477D)* was injected into both *dpy-5(e907)/dpy-5(e907)* individuals and into a DAF-28::GFP reporter background strain (VB1605; svIS69), generously provided by Simon Tuck (Kao et al. 2007) and Marco Gallo. Strains generated: BC8561; sEX2254 *dpy5(e907)/dpy5(e907) [ZK829.4(G477D)::pBluescript + pCeh361 + pCFJ104]*, and BC8564; sEX2254 *DAF-28::GFP (VB1605; svIS69) [ZK829.4(G477D)::pBluescript + pCeh361 + pCFJ104]*. PCR using a *ZK829.4*-specific forward primer (`AGAAC CGCTG GATTC ACCTT`), and a *pBluescript*-specific reverse primer (M13R) was performed to ensure the presence of the *ZK829.4(G477D)::pBluescript* construct in the transgenic organisms.

4.2.3 Microscopy

See section 1.2.10 Materials and methods for a detailed description on microscopy. GFP and mCherry expression pattern analysis was done using a Zeiss Axioscope equipped with a QImaging camera and the appropriate GFP or RFP filters. All GFP images were taken under identical filter, lens, and camera settings. All mCherry images were also taken under identical filter, lens, and camera settings. Exposure times are indicated on the figures.

4.3 Results

A mutation in the negative allosteric domain of GDH was created via DpnI site-directed mutagenesis to determine the effects of loss of GTP-binding on insulin regulation by GDH. As seen in Figure 14, DAF-28::GFP expression in the ASI and ASJ neurons of the head increased in the presence of the *ZK829.4(G477D)* mutant construct.

4.4 Discussion

In humans, mutations inhibiting the negative allosteric regulation of glutamate dehydrogenase by GTP results in a unique hyperinsulinism/hyperammonemia syndrome due to increased α-ketoglutarate and ammonia production by GDH (Stanley et al. 1998). Due to the homohexameric nature of GDH, the GTP-binding site mutations are able to act dominantly, and thus represent gain-of-function mutations. To determine whether *C. elegans* glutamate dehydrogenase has a similar role in insulin regulation, and whether it is also inhibited by GTP, I created a GDH transgene construct with a mutation affecting the GTP-binding site (*ZK829.4(G477D)*), which was injected directly into a DAF-28::GFP background. DAF-28 is a beta-insulin expressed in the ASI and ASJ neurons of the head, and that is homologous to human insulin.

Introduction of the *ZK829.4(G477D)* transgene into a DAF-28::GFP reporter background resulted in increased GFP expression in the ASI and ASJ neurons (Figure 14). From these results, I conclude that *C. elegans* GDH is also able to regulate insulin levels analogously to human GDH, and that GTP is a negative allosteric regulator of *C. elegans* GDH. In *C. elegans*, increased insulin/IGF-1 receptor-like signalling stimulated by DAF-28 inhibits dauer arrest (Li et al. 2003). Dauer is an alternative larval developmental stage induced by non-favourable environmental conditions, such as over-

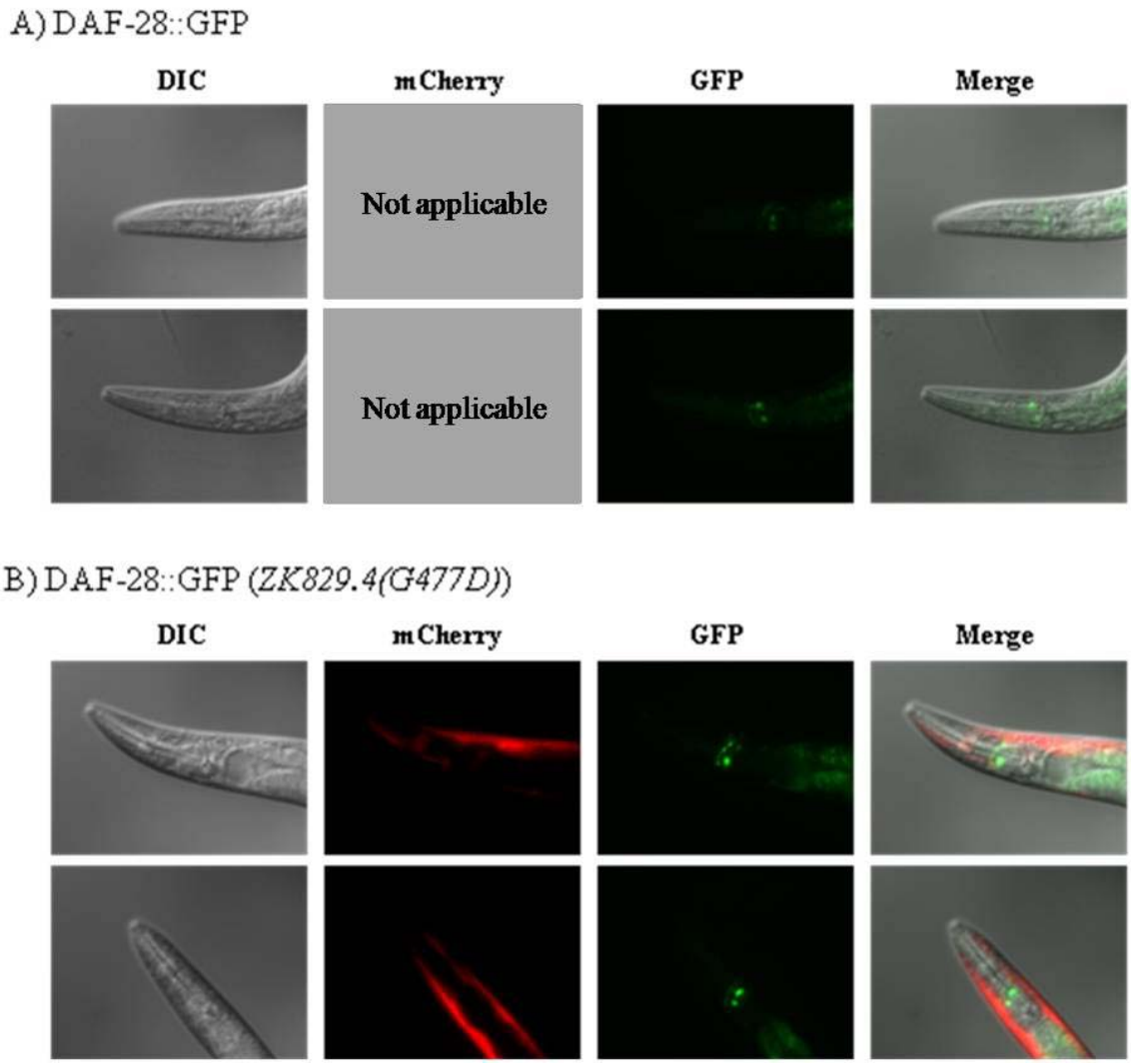

Figure 14. DAF-28::GFP expression levels in the absence and presence of the *ZK829.4(G477D)* mutant construct

The expression of DAF-28::GFP in the ASI and ASJ neurons increases in the presence of the *ZK829.4(G477D)* mutant transgene (B), compared to in wildtype worms (A). Exposure times are as follows: mCherry – 250ms, GFP – 3000ms. All nematodes imaged were at the young adult stage, based on extent of gonad and vulval development, to ensure their levels of expression were relatively equivalent.

crowding, starvation, or high temperature. Dauer larvae are able to survive better under these harsh conditions due to special adaptive features, such as thicker cuticles, constricted pharynxes, intestinal fat retention, transcriptional quiescence, resistance to metabolic stress, and extended lifespan. Under normal conditions, insulin signalling by DAF-28 triggers the inhibition of DAF-16, a forkhead transcription factor that transcribes genes necessary for dauer formation, by promoting its retention in the cytoplasm (Ogg et al. 1997). Since increased glutamate dehydrogenase activity results in increased insulin signalling through DAF-28, it is likely that loss of allosteric inhibition of GDH by GTP also inhibits dauer arrest. Determination of a dauer-defective phenotype in transgenic nematodes with the *ZK829.4(G477D)* mutated transgene would further confirm the role of GDH in regulating insulin in *C. elegans*.

Loss of GTP binding in human GDH leads to a double phenotype of hyperinsulinism and hyperammonemia, indicating that increased GDH activity also affects nitrogen metabolism. It would be interesting to determine whether *C. elegans* GDH has a similar role in the production of ammonia, the main metabolic waste product of nitrogen.

Glutamate dehydrogenase is an extremely well conserved metabolic gene, whose actions are closely orchestrated with energy levels, amino acid catabolism, and carbon and nitrogen metabolism. Due to the central nature of this protein, not only has its function been conserved across evolution, but so has its intricate modes of regulation, as demonstrated by increased DAF-28 production upon introduction of a GTP-binding site mutant of GDH into *C. elegans*.

GENERAL DISCUSSION

This thesis has focused on the molecular identification and regulatory characterization of the essential gene, *let-56*, in *Caenorhabditis elegans*. Essential genes by nature and definition are central to the survival and fecundity of an organism, and are generally evolutionarily well conserved across multiple species. Consequently, the study of these fundamental genes in *C. elegans* allows us to better understand their human homologs, mutations in many of which result in diseases.

In Chapter 1, I determined the molecular identity of *let-56* by sequencing the *ZK829.4* region in seven of twelve alleles. *ZK829.4* was previously identified as a candidate for the identity of *let-56* by the work of S.S. Prasad, D.V. Clark, and M.A. Marra (Prasad and Baillie 1989; Clark and Baillie 1992; Marra 1994). Sequencing identified G/C to A/T mutations in all seven alleles, corresponding to treatment with EMS, and resulted in amino acid changes in well conserved residues (*s46*, *s50*, *s168*, *s173*, *s1192*, *s1223*, and *s2230*), or a truncated protein (*s168*) (Figure 3). *ZK829.4* corresponds to glutamate dehydrogenase, a mitochondrial matrix protein that plays a central role in carbon and nitrogen metabolism. Considering the well-conserved nature and function of GDH, it is unsurprising that it is such a large target for mutagenesis, since most amino acid changes could alter the structure and/or function of the protein. In this section I also determined the lethal arrest stage of *let-56(s173)* homozygote mutants to correspond to early larval based on the extent of gonadal development (Kimble and Hirsh 1979) after 2 weeks at 20˚C (Figure 2), contrary to previous results obtained by M.A.

Marra and D.V. Clark (Clark 1990; Clark and Baillie 1992; Marra 1994). Differences in arrest stage compared to Clark's results (mid- to late-larval lethal) are attributed to the mechanism of scoring, as she based arrest stage on the relative length of the worm compared to WT nematodes (Clark 1990; Clark and Baillie 1992). However, since both Marra and I scored arrest stage based on gonadal development, differences could be due to additional mutations accrued in the *let-56(s173)* strain I used for my assay that further affect the health of the worm. In this instance, it is possible that waiting longer than two weeks could give rise to a sterile adult.

Elucidating mechanisms of gene regulation provide us with a better understanding of the basic functionality of the gene. For example, knowing the tissue-specific expression pattern of a gene could give us valuable information on how it is involved in the differentiation of those cell types. There are multiple levels of gene regulation: pre-transcriptional, transcriptional, translational, and post-translational. At the pre-transcriptional level, gene expression is regulated by overall chromatin structure which dictates how available a specific locus is to the transcription machinery. At the transcriptional level, expression is regulated by transcription factors, such as activators and repressors, which can indirectly modify the strength of association between RNA polymerase and the promoter. Besides modifying the level of a gene's expression, tissue-specific or stage-specific transcription factors can also influence the spatial or temporal expression of a gene. Translational regulation occurs at the level of the mRNA, and can include miRNA binding sites in the 3' untranslated region, binding of repressor proteins to mRNA, or modulation of the initiation factors required for mRNA translation at the ribosome. Post-translationally, protein expression and/or activity can be regulated by

covalent modifications (e.g., phosphorylation, ubiquitination), proteolysis, or the action of coenzymes, inhibitors, or activators, amongst other regulatory mechanisms. In this thesis, I characterized some of the mechanisms of GDH control in *C. elegans*.

In Chapter 2, I examined the translational regulation of *ZK829.4* by attempting to determine a *cis*-regulatory motif in the upstream promoter region. This was done by performing sequential promoter::GFP cut downs. Reporter constructs were injected into the worm and then analyzed for the presence or absence of fluorescence. Since GDH has a complex expression pattern, I simplified my analysis by looking for complete loss of GFP rather than loss in a few tissues. Consequently, I identified a 31bp window likely to contain a TF binding site necessary for *ZK829.4* expression. Inspection of this region using TESS (Transcriptional Element Search Software) found three predicted *cis*-regulatory elements in this area, corresponding to STE12, GATA-1, and Sp1 (Figure 5, Table 3). Since STE12 is only found in Saccharomycetaceae, it was removed as a possible factor. The *C. elegans* homolog for GATA-1, *end-1*, is involved in endoderm formation (Zhu et al. 1997). Since nutrient processing occurs in the gut, it is possible that there is a greater need for GDH within this tissue type, and that this increased expression is driven by END-1. Sp1 is involved in early embryo development, and has recently been implicated in the regulation of genes in response to insulin (Solomon et al. 2008). Alternatively, it is possible that this region contains a novel transcription factor specific to the genus *Caenorhabditis*, since the extent of sequence conservation between *C. elegans* and *C. briggsae* is high in this region (Figure 5). A series of finer promoter truncations in this region (e.g., every 5 bp) would provide more conclusive results as to

the exact location of the putative *cis*-regulatory motif, since it would significantly narrow the search window and eliminate extraneous results.

In Chapter 3 I evaluated the importance of the 3' UTR of *let-56* in the regulation of GDH expression. Two computational prediction programs, miRanda and PicTar, have predicted multiple miRNA binding sites to exist in the 3' UTR of *ZK829.4* (Figure 7), which have yet to be validated. In addition, the *ZK829.4* gene models indicate that there are two transcripts of the 3' UTR, one spliced and one unspliced, that differ in their miRNA binding sites (Figure 7). To determine whether the 3' UTR played any role in regulating gene expression, I generated chimeric GFP reporter constructs driven by the endogenous *ZK829.4* promoter region and differing in the attached 3' UTRs. The *unc-54* 3' UTR was used as a control, since it acts as an mRNA stabilizer and is used for most promoter::GFP reporter constructs in *C. elegans*. From this analysis, I determined that the 3' UTR of *ZK829.4* does affect the level of expression, as well as the spatial pattern, since the level and extent of fluorescence inversely correlated with the number of predicted miRNA binding sites available on the attached 3' UTR (Figure 11). qRT-PCR analysis to check for stage-specific differences in expression levels of the two 3' UTR transcripts confirmed these results, and also indicated that there may be stage specific differences in the expression pattern for the two transcripts (Figure 10). Based on these results, I conclude that the 3' UTR may also play a role in the temporal regulation of GDH expression. Further analysis can be done by testing each of the predicted miRNA binding sites via site-directed mutagenesis. Validation would not only provide a more detailed analysis on the regulatory control of the 3' UTR, but it would also strengthen predictor programs such as miRanda and PicTar.

In Chapter 4 I analyzed a post-translational aspect of *let-56* regulation. Mature GDH functions as a homohexamer and has both negative (GTP) and positive allosteric (ADP, leucine) regulators. Mutations in the GTP-binding site of human GDH result in hyperinsulinism/hyperammonemia (HI/HA) syndrome. Research by Stanley et al. (1998) has shown that individuals with HI/HA are genotypically heterozygous, indicating that the mutation functions in a dominant manner. To determine whether *C. elegans* GDH has a similar role in the regulation of insulin levels, and if it regulated by GTP in an analogous manner, I generated a *let-56* mutant construct mimicking a commonly found mutation in HI/HA patients (Stanley et al. 1998). This construct was injected directly into a DAF-28::GFP background (Kao et al. 2007), on the assumption that it would also act in a dominant manner. DAF-28 is a beta-type insulin and a homolog of human insulin. Presence of the *ZK829.4(G477D)* construct resulted in increased DAF-28::GFP fluorescence, indicating that it was able to increase the production of insulin specifically due to the loss of GTP binding (Figure 14). From these results I conclude that *C. elegans* GDH functions in a similar mechanism as human GDH. This analysis can be strengthened by screening for increased ammonia production in these mutants, and for a dauer defective phenotype, since increased signalling by DAF-28 inhibits dauer formation.

APPENDICES

Appendix A. *let-56* strains used for sequence analysis.

Strain	Genotype
BC3488	*let-56(s46) unc-22(s7)/nT1(IV);+/nT1(V) [let- (m435)* on *nT1]*
B03489	*let-56(s50) unc-22(s7)/nT1(IV);+/nT1(V) [let- (m435)* on *nT1]*
BC3490	*let-56(s168) unc-22(s7)/nT1(IV);+/nT1(V) [let- (m435)* on *nT1]*
BC3491	*let-56(s173) unc-22(s7)/nT1(IV);+/nT1(V) [let- (m435)* on *nT1]*
BC3492	*let-56(s1192) unc-22(s7)/nT1(IV);+/nT1(V) [let- (m435)* on *nT1]*
BC3494	*let-56(s1223) unc-22(s7)/nT1(IV);+/nT1(V) [let- (m435)* on *nT1]*
BC4436	*let-56(s2230) unc-22(s7) lev-1(x22)/nT1(IV);+/nT1(V) [let- (m435)* on *nT1]*

Appendix B. ZK829.4 wildtype sequence and primers used for sequencing of *let-56* alleles.

>*ZK829.4* (*IV*: 11952772,11955824)

cgtccccaggacgagcttttcgtggcctagaagcgtttgcctactcgcgggcggtgccacatttt
ttttaggaaaaaaggttttgatgcctctgccaatttttttgatttaaatatttttaaacgagct
ataacttaaataatttcaaactgccgctgaaaattattaaaggcgcatggatttcgtgacgagac
ctcctggcattttccttacttttcgattccgcccggatcttttcctccttttgcactttggctt
cttatgtaaaatctcttatttgtttaaattttaattacaaaatattttattttcaggtaatgttg
agcactctttccagaggcgcccgctcggtcgctgtccgaagctattcggccgctactctcgatgc
ccactcccaggtgctcgacgagcagaagccaatggaggagcaggtcaacccatctttctacaaga
tggtcgacttttacttcaacaagggagccgaggtcatcgctccaaaactcgccgaggagctcaag
tccaactctttgagccaaaaggataagaagaatctcgtgtccggaattcttggagctatcaagcc
agttaacaaggtaagaattttgagtctcattaatttatcatattttatttcttcaggtccttta
catcaccttcccaatccgtcgtgacaatggagagttcgaggttattgaggcctggcgcgcacagc
attctgagcacagaactccaaccaagggaggtatccgttattccctcgatgtgtgcgaagatgag
gtcaaagctttgtctgctcttatgacttacaagtgcgctgttgtcgatgttccattcggaggagc
taagggaggagtcaagattgatccaaagcaatacactgattatgaaattgagaagatcacccgcc
gtatcgctatcgaattcgcaaagaagggattcctcggccccggagttgatgtcccagccccagat
atgggaaccggagagcgtgaaatgggatggatcgctgatacctacgcccaaaccattggacattt
ggacagagtgagtataaatttttgtgagcatgtgaataattttgtttgcaggatgcttcggctt
gtatcacaggaaagccaattgtcagtggaggaattcacggacgtgtttccgccaccggacgtgga
gtgtggaagggactcgaggtgttcaccaacgatgctgattacatgaagatggtcggtcttgacac
cggactcgctggaaagactgctatcatccaaggattcggaaacgtcggacttcacacccacagat
acctccaccgtgctggatcaaaggtcatcggaatccaggagtacgattgcgccgtctacaaccca
gatggtattcatccaaaggagctcgaagattggaaggacgccaatggaactatcaagaacttccc
aggagccaagaacttcgacccattcactgagcttatgtacgagaagtgcgatatcttcgttccag
ctgcttgcgaaaagtcgatccacaaggaaaatgctagccgcattcaagctaagatcatcgccgag
gctgccaacggaccaactaccccagctgctgacagaattcttcttgctcgtggagattgcctcat
catcccagacatgtacgtcaactctggtggagttactgtttcctacttcgagtggttgaagaatc
ttaaccatgtttcctacggacgtcttacattcaaatatgacgaggaagccaacaagatgcttttg
ggtaagtaaattttcgaaatttgaattcctagacttgcgtagagtaacacaatgaaacgatttgc
aagttttcatctgtgataaaatttgtttagaaactaacaagggctagatactcttacgcttgtc
acacttttccgtttattttatgaggagggagaggaggccactcaaccgttgtcgtgaaaatgagt
acgtatgcactctaggaaacaaattgtaaatcaattctttctgtttaaaaatgtttgaattttca
gcctcggtccaagaatctctctccaaggccgtcggaaaggattgcccagttgaaccaaatgctgc
tttcgctgccaagatcgctggagcttccgagaaagacatcgttcactctggactcgagtacacaa
tgcaacgctccggagaagccatcatccgcaccgctcacaagtacaaccttggacttgatatccgt
actgctgcctatgccaactccatcgagaaggtctacaacacctacagaaccgctggattcacctt
cacataa*gtacccacttctcactcatctcatggctcttgtatcctcttttatgacatcaaatggc*
tccaagccaggtttaaatagcttcgtgtaacccttagtgccttttccatagttttctgtttcga
aactatctaggttaactaaagtctagctctgatcttttctgcctggttcgttctcactttagtat
aattaaatattttattggttccccacccctttcatccccacacataatttttcgttgtttgtt
ggttcgggacggtttcgagacggagaccattcttcaaaaaaaaatctcaaaaataataaaaagtt
*tatttcctt*aaacacttctacatggtcattgcaattttccaatgatcattggaaaagaaatttca
gggagcattaaaaactttatcagacttgtgtctttctatttactataatttagaattttcgataa
catatcactttcacattgtgtgccactatcagcttcaaatttgggaatcacctccacaattgttg

Underlined: gene *Italicized*: 3′ untranslated region

Sequencing Primer	Sequence
Forward-1	cctttttgcactttggcttc
Forward-2	gtgtgcgaagatgaggtcaa
Forward-3	gactcgctggaaagactgct
Forward-4	acgaggaagccaacaagatg
Forward-5	cacctacagaaccgctggat
Reverse-1	cggctcccttgttgaagtaa
Reverse-2	tatcagcgatccatcccatt
Reverse-3	agcattttccttgtggatcg
Reverse-4	cttggaccgaggctgaaaat
Reverse-5	tgcaatgaccatgtagaagtgtt

Appendix C. Forward primers used for *let-56* promoter amplification for *let-56*$_{promoter}$::GFP transgene constructs

Distance from ATG start site (bp)	Forward primer
-593	CACAATATGGGCGAAGATCA
-588	TATGGGCGAAGATCAATGAC
-583	GCGAAGATCAATGACACTCG
-578	GATCAATGACACTCGTCCCA
-573	ATGACACTCGTCCCACTCTTC
-563	TCCCACTCTTCTTTTTTCCTTC
-558	CTCTTCTTTTTTCCTTCTTCAAAT
-553	CTTTTTTCCTTCTTCAAATAGGC
-548	TTCCTTCTTCAAATAGGCGG
-543	TCTTCAAATAGGCGGAGCAT
-445	CCTCCTCCATGAAACGCTAT
-414	AGTTTCATCGGTCTCGCCC
-363	GTTTTGTGTTGGGCTCCTCT
-78	CCTTTTTGCACTTTGGCTTC

Appendix D. *ZK829.4*$_{\text{promoter}}$::GFP strains

Strain	Genotype
BC7858; sEX1734	*dpy-5(e907)/dpy-5(e907)[ZK829.4*$_{promoter(-593)}$*::GFP+pCeh361]*
BC7859; sEX1735	*dpy-5(e907)/dpy-5(e907)[ZK829.4*$_{promoter(-445)}$*::GFP+pCeh361]*
BC7860; sEX1736	*dpy-5(e907)/dpy-5(e907)[ZK829.4*$_{promoter(-363)}$*::GFP+pCeh361]*
BC7861; sEX1737	*dpy-5(e907)/dpy-5(e907)[ZK829.4*$_{promoter(-78)}$*::GFP+pCeh361]*
BC8321; sEX2026	*dpy-5(e907)/dpy-5(e907)[ZK829.4*$_{promoter(-543)}$*::GFP+pCeh361]* (segI)
BC8559; sEX2252	*dpy-5(e907)/dpy-5(e907)[ZK829.4*$_{promoter(-543)}$*::GFP+pCeh361]* (segII)
BC8322; sEX2027	*dpy-5(e907)/dpy-5(e907)[ZK829.4*$_{promoter(-414)}$*::GFP+pCeh361]*
BC8515; sEX2211	*dpy-5(e907)/dpy-5(e907)[ZK829.4*$_{promoter(-588)}$*::GFP+pCeh361]*
BC8516; sEX2212	*dpy-5(e907)/dpy-5(e907)[ZK829.4*$_{promoter(-583)}$*::GFP+pCeh361]*
BC8517; sEX2213	*dpy-5(e907)/dpy-5(e907)[ZK829.4*$_{promoter(-578)}$*::GFP+pCeh361]* (segI)
BC8560; sEX2253	*dpy-5(e907)/dpy-5(e907)[ZK829.4*$_{promoter(-578)}$*::GFP+pCeh361]* (segII)
BC8518; sEX2214	*dpy-5(e907)/dpy-5(e907)[ZK829.4*$_{promoter(-573)}$*::GFP+pCeh361]*
BC8520; sEX2216	*dpy-5(e907)/dpy-5(e907)[ZK829.4*$_{promoter(-563)}$*::GFP+pCeh361]*
BC8521; sEX2217	*dpy-5(e907)/dpy-5(e907)[ZK829.4*$_{promoter(-558)}$*::GFP+pCeh361]* (segI)
BC8526; sEX2221	*dpy-5(e907)/dpy-5(e907)[ZK829.4*$_{promoter(-558)}$*::GFP+pCeh361]* (segII)
BC8522; sEX2218	*dpy-5(e907)/dpy-5(e907)[ZK829.4*$_{promoter(-553)}$*::GFP+pCeh361]*
BC8523; sEX2219	*dpy-5(e907)/dpy-5(e907)[ZK829.4*$_{promoter(-548)}$*::GFP+pCeh361]*

Appendix E. *C. elegans ZK829.4* and *C. briggsae* ortholog promoter sequences

C. elegans
>IV:11952045,11953262 (-1167 to +50)

actttcgatttatgcttatgtctagatttatccggtttcaaattactaacctgtttttctttttt
atcacaactaacaagctcacgttttatcattcttgaaatttttttcaataaataatgaaaataaaa
tcaaaagtgtagaatttgttcttaaaggcgcatgaattcattccaatgggtctcgtcgggagaaa
aagtttatggtagcgcgtcttggtgctcggatttttttaattatttttttttccatttttaaaaatat
tttatgctctatgtttggttatggaagcgaccaccgaaaaagccacattcttcaaaaatttctgt
caaatctctgggggagaaataaaatttaaaaatcggttgtcttattctgaagattatttacgaag
aatcaaagatgtcgatcagtaaaacaaatcgaaagagaaacaaaaacaaaactggtattcaaaat
tcgttgaatgagatttttgacgcgaatttagcgagacactgtctcgattctttctcagatgacgt
cgattgaccctgcttcttttgttttgttgctatgcagatcgtatgtcctatgcaatagcaccaca
caatatgggcgaagatcaatgacactcgtcccactcttctttttttccttcttcaaataggcggag
catcttttctctatttttcccccgaatgttgcctctatttctctctttctctaaatatctatttg
ccagtcacctcctcctcctcctccatgaaacgctatcttttgcttgcagtttcatcggtctcgcc
caccgatgatggttgcgcgttgtcctgtaaacagttttgtgttgggctcctctagttttgaatag
ttatggcgcccgcgtccccaggacgagctttcgtggcctagaagcgtttgcctactcgcgggcg
gtgccacatttttttttaggaaaaaaggttttgatgcctctgccaatttttttttgatttaaatatt
tttaaacgagctataacttaaataatttcaaactgccgctgaaaattattaaaggcgcatggatt
tcgtgacgagacctcctggcattttccttacttttcgattccgcccggatcttttcctcctttttt
gcactttggcttcttatgtaaaatctcttatttgtttaaatttttaattacaaaatattttatttt
caggtaatgttgagcactctttccagaggcgcccgctcggtcgctgtc

C. briggsae
>IV:4980047,4981264 (-1167 to +50)

ttattagtaaagattcataaatttgttcaggtgacaattaattataggaattccgtatccttcca
gtcaaatttgtgtcagaatagatctgtggaaaagttatttctacattcccgttcttctcttgcct
gaaagatatttcctttacaaatttgttaactgcagttcactgaataatatctaggttatcaagaa
tatattcctccagtcaatctgaatatatcgtattacattttcatacaactggaactagaaatttt
ttcgtaaacttttttgttcagaagtatacaattgaaaactgataactgtgagttgagaggaagtg
aaacagaaagttttgaaaaaaaattttttgatccagaaatgacagcaacgaagatcagattttgag
atcatgaaacaaatatttttcagaaacatacatcaacaatagtcattcattgaatgagatttgat
atgacatgaaacaaacgaaaaaataatgtttccttcttgtttttcctgatgacgtcgtctaaata
gtcttcttctgtttcgttgctatgcggattgccctctctatacagcacacacgtccatcgtcgac
atgaacgaagatcaatgacacactcgttgcgctcttttcttcatcttcttcagagggcggagttt
tctttttctttttttatgtttttttttttctcgccgccccaacttcctctttttctctatctctgt
ttcccactcacccctcccctgaaacgctatcgtttgcttgcagtttcgttagtttcgccctctga
cgatggttgcgcgttgtcctgtaaacagtatagtgttggctcccctcggttgcttcgtggcgccc
gcgtccctgggcctagcttttcgtggcctagaaaactttgcataaattcgggcgacacctaaatt
ttgggatttacttttgctgctcttctctctattctagattgcttcttgaccggtttggctgaaa
aatctaaaaataggtctgacttttttttaattttaaacttccgctcaaagaaaactcaaaggccaa
gtctgtcgctgcgggacccaccagtcttctttttccgaactcgctttttttgcataacctcattcg
aatttctcacgatttcgatgatgttccagtagtttttttttgcaaatatctaattttcaggtaa

Appendix F. *ZK829.4*$_{promoter}$::GFP expression analysis

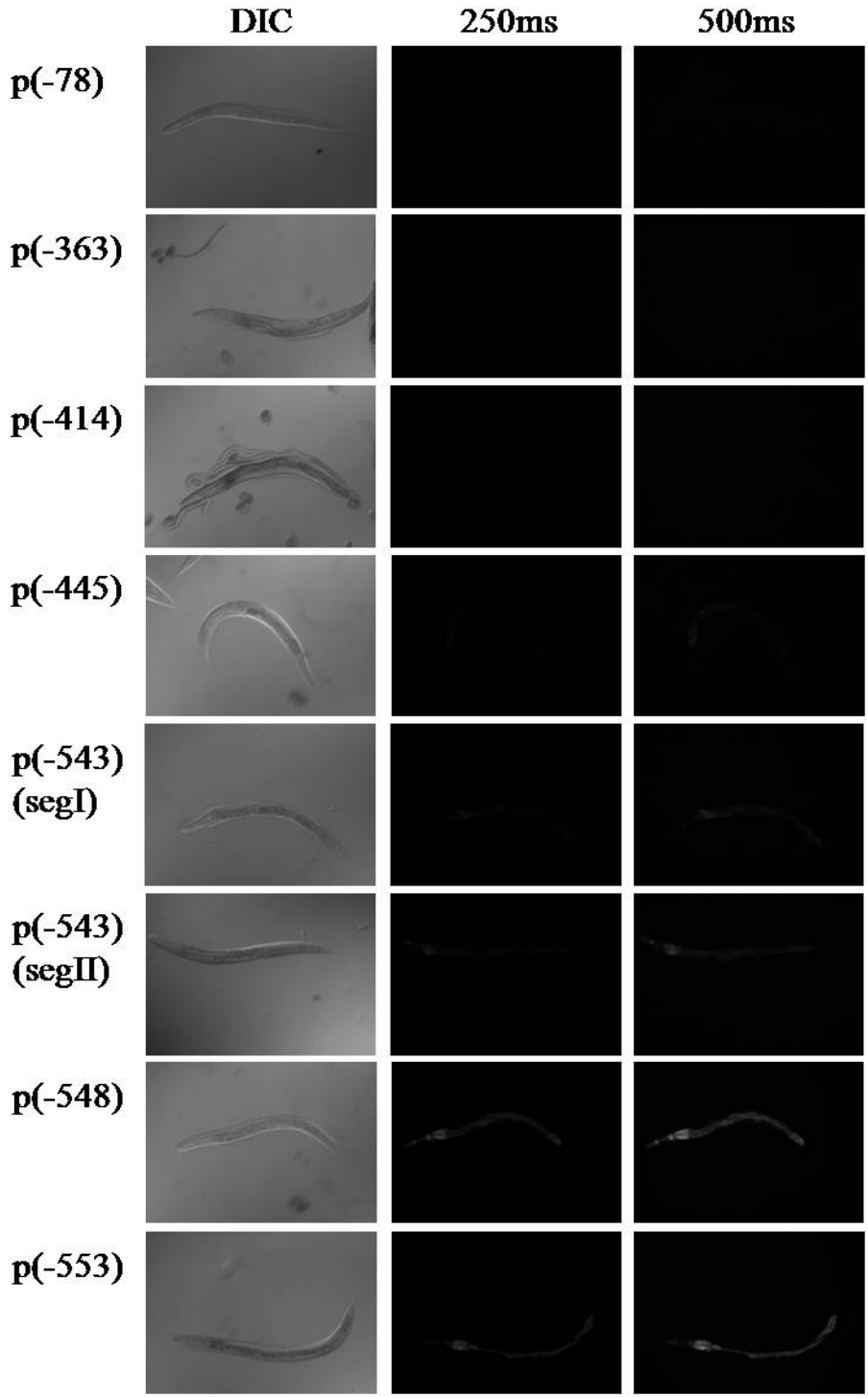

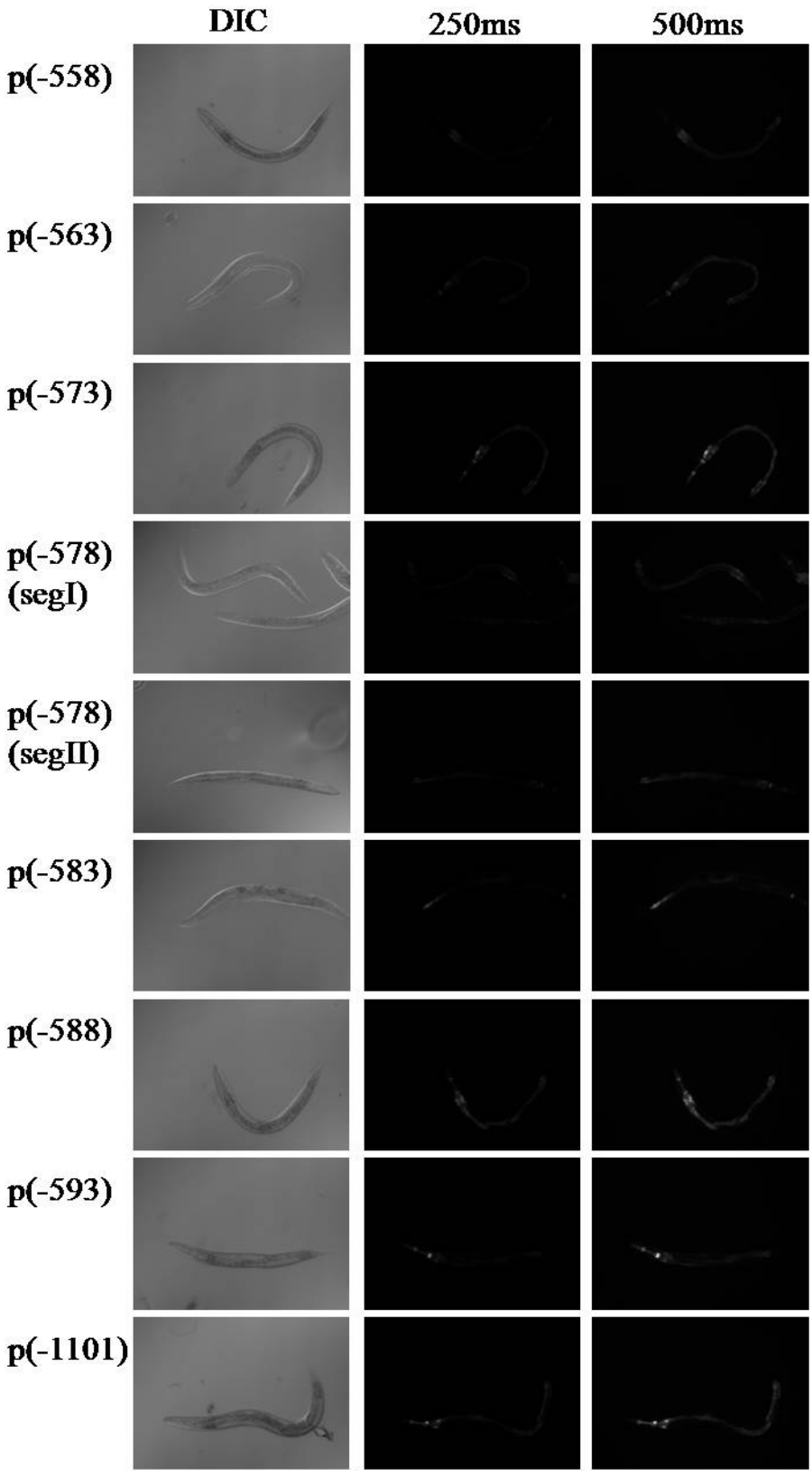
DIC
250ms
500ms
p(-558)
p(-563)
p(-573)
p(-578)
(segI)
p(-578)
(segII)
p(-583)
p(-588)
p(-593)
p(-1101)

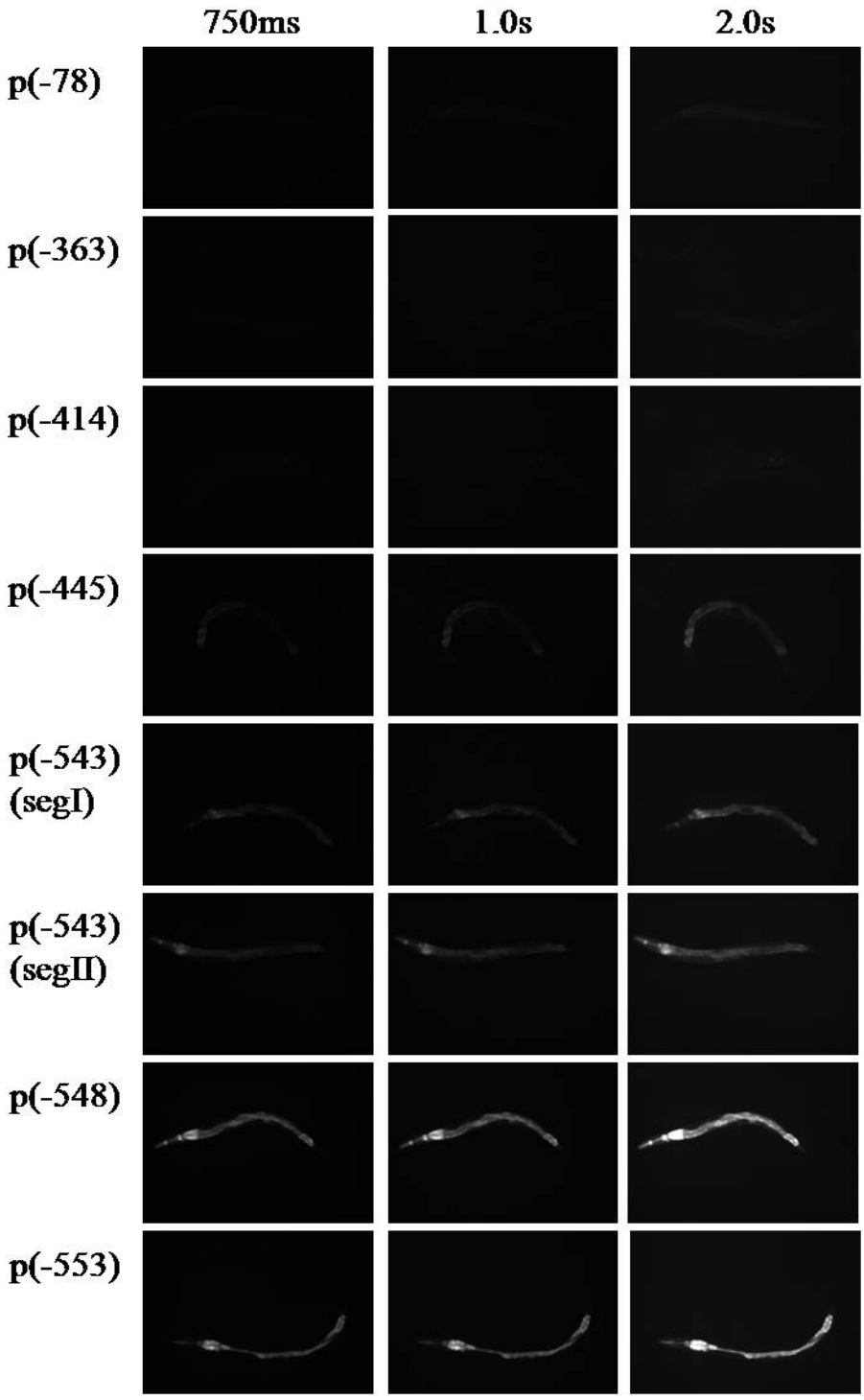
750ms
1.0s
2.0s
p(-78)
p(-363)
p(-414)
p(-445)
p(-543)
(segI)
p(-543)
(segII)
p(-548)
p(-553)

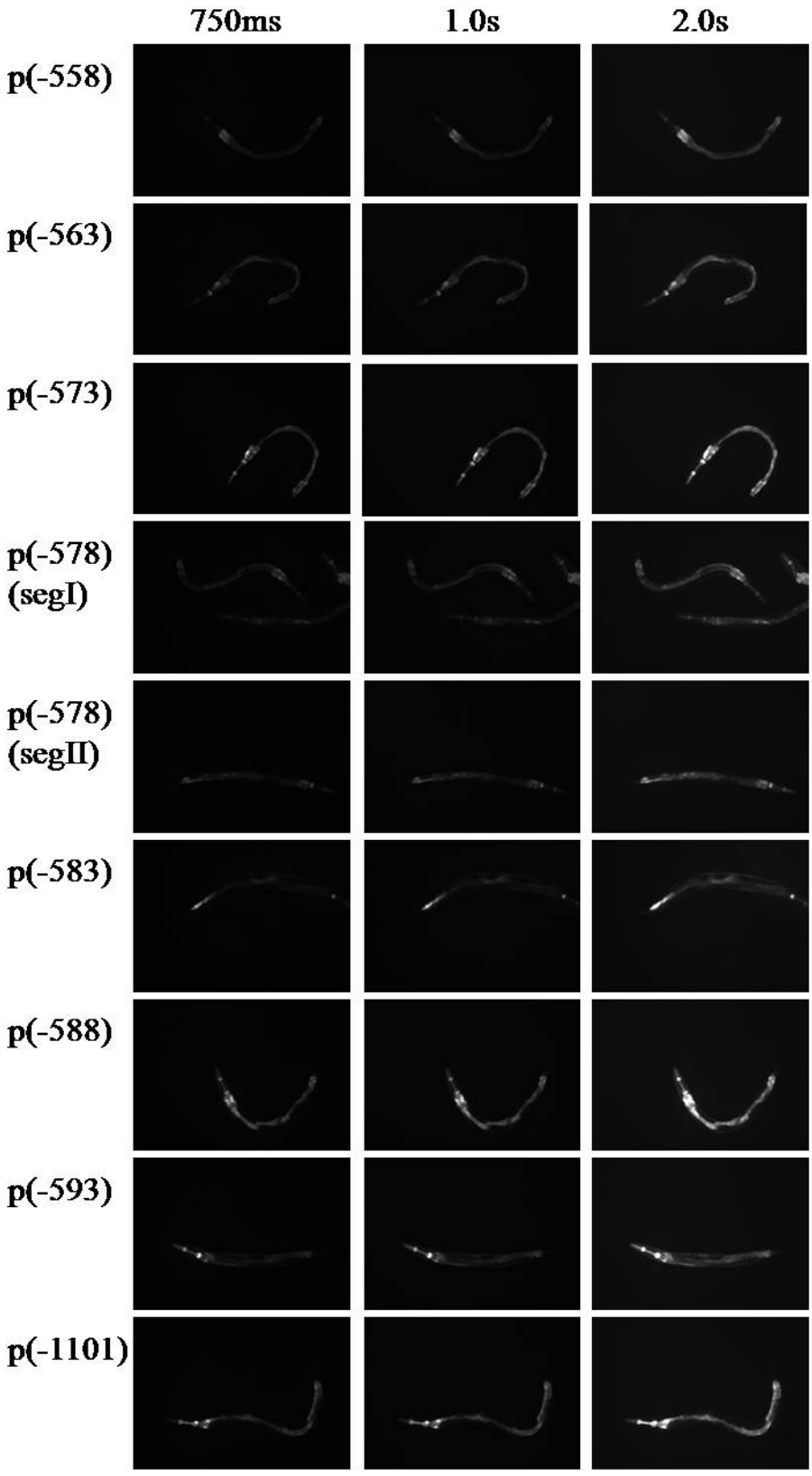
750ms
1.0s
2.0s
p(-558)
p(-563)
p(-573)
p(-578)
(segI)
p(-578)
(segII)
p(-583)
p(-588)
p(-593)
p(-1101)

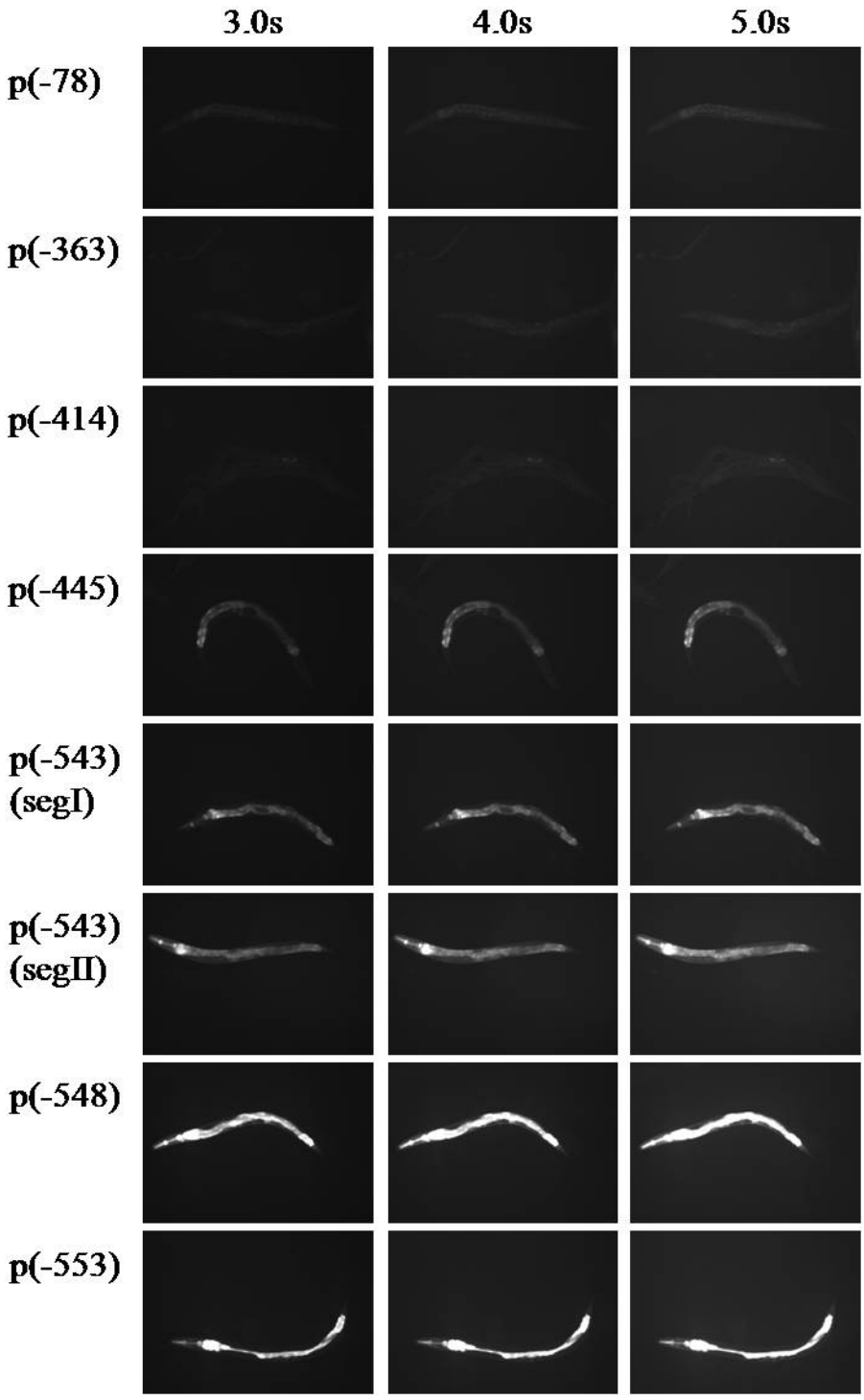
3.0s
4.0s
5.0s
p(-78)
p(-363)
p(-414)
p(-445)
p(-543)
(segI)
p(-543)
(segII)
p(-548)
p(-553)

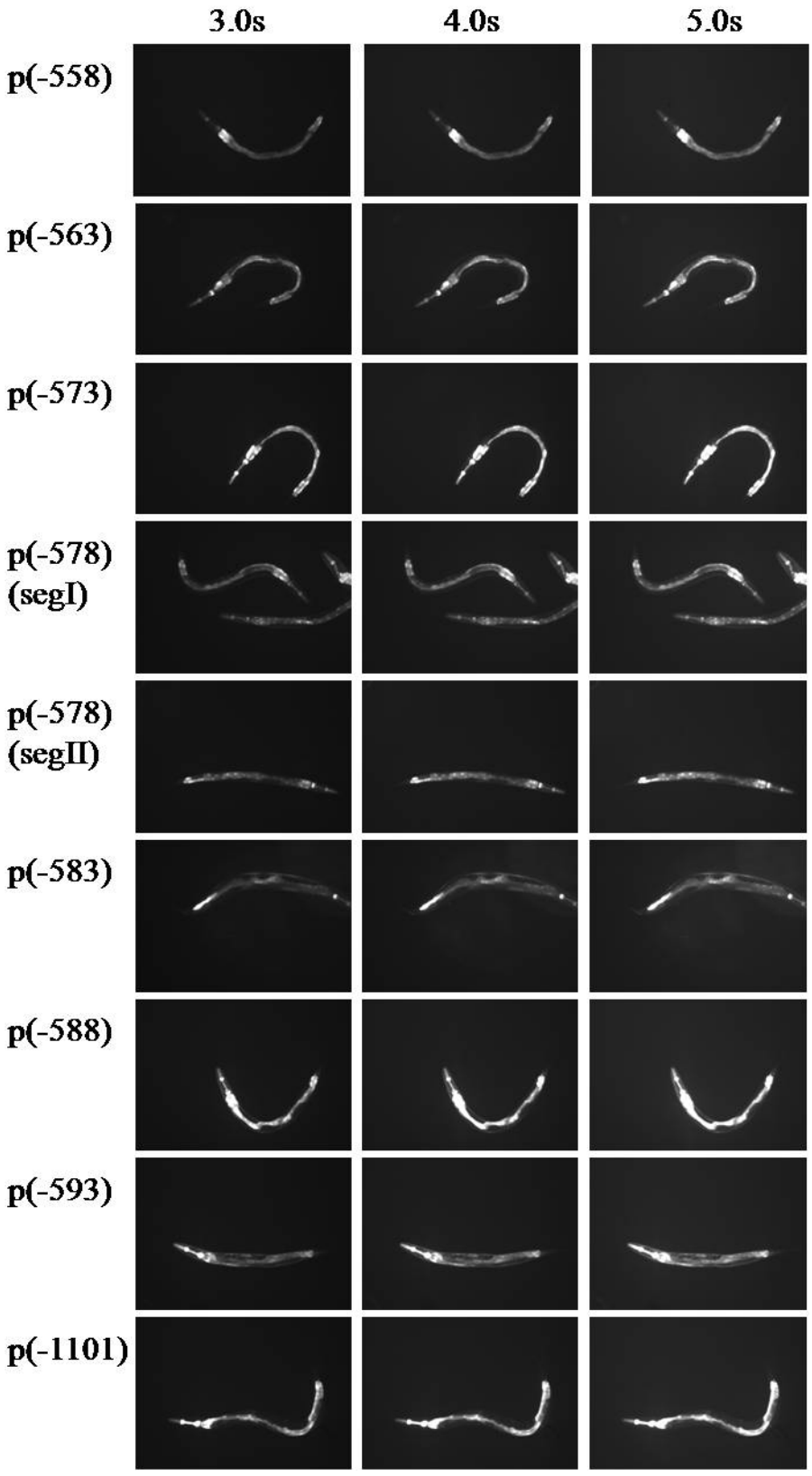
3.0s
4.0s
5.0s
p(-558)
p(-563)
p(-573)
p(-578)
(segI)
p(-578)
(segII)
p(-583)
p(-588)
p(-593)
p(-1101)

Appendix G. ZK829.4$_{promoter}$::GFP::3' UTR strains

Strain	Genotype
BC8180; sEX1902	*dpy-5(e907)/dpy-5(e907)[ZK829.4$_{promoter(-1101)}$::GFP::ZK829.4 3' UTR$_{whole}$+pCeh361]*
BC8181; sEX1903	*dpy-5(e907)/dpy-5(e907)[ZK829.4$_{promoter(-1101)}$::GFP::unc-54 3' UTR +pCeh361]*
BC8519; sEX2215	*dpy-5(e907)/dpy-5(e907)[ZK829.4$_{promoter(-1101)}$::GFP::ZK829.4 3' UTR$_{spliced}$+pCeh361]*
BC8525; sEX2220	*dpy-5(e907)/dpy-5(e907)[ZK829.4$_{promoter(-1101)}$::GFP::ZK829.4 3' UTR$_{variant}$+pCeh361]*
BC8565; sIS1903	*dpy-5(e907)/dpy-5(e907)[ZK829.4$_{promoter(-1101)}$::GFP::unc-54 3' UTR +pCeh361]*

Appendix H. qRT-PCR results and sample calculation

	Sample Detected								
Stage	***rpl-19***			**3'UTR whole**			**3' UTR spliced**		
L1-s	17.72	17.85	17.91	18.51	18.45	18.39	16.00	16.12	16.87
L1	19.61	19.40	20.44	22.48	22.24	22.40	19.93	20.08	19.93
L2	19.04	19.41	18.96	22.73	20.43	22.61	20.11	20.21	20.20
L3	17.13	16.60	16.85	14.70	19.33	19.20	16.74	16.94	16.80
L4	17.29	16.67	17.40	19.17	18.99	19.03	17.74	17.63	17.63
Adult	17.76	17.85	16.66	18.98	19.66	20.50	17.88	17.92	17.66

= Outliers removed prior to analysis

Note: Values in table refer to cycle numbers (C_T).

The ΔC_T Method using a Reference Gene was performed according to support data provided by BioRad (http://www.bio-rad.com). The ΔC_T method is a variation of the Livak method that uses the difference between sample and reference C_T values to determine differences in expression levels between samples.

Sample calculation using L1-s stage data:

The formula for expression is: $\text{Expression} = 2^{(C_T(\text{ref}) - C_T(\text{sample}))}$

Expression (3' UTR whole):

Trial I: $2^{(17.72 - 18.51)} = 0.578$

Trial II: $2^{(17.85 - 18.45)} = 0.660$

Trial III: $2^{(17.91 - 18.39)} = 0.717$

Average expression: 0.652 Standard deviation: 0.070

Expression (3' UTR spliced) $= 2^{(17.83 - 16.33)} = 2.82$

Trial I: $2^{(17.72 - 16.00)} = 3.29$

Trial II: $2^{(17.85 - 16.12)} = 3.32$

Trial III: $2^{(17.91 - 16.87)} = 2.06$

Average expression: 2.89 Standard deviation: 0.72

These average expression values and standard deviations were graphed for each developmental stage to give the graph seen in Figure 10.

REFERENCE LIST

Barriere, A., S. P. Yang, et al. (2009). "Detecting heterozygosity in shotgun genome assemblies: Lessons from obligately outcrossing nematodes." Genome Res **19**(3): 470-80.

Betel, D., M. Wilson, et al. (2008). "The microRNA.org resource: targets and expression." Nucleic Acids Res **36**(Database issue): D149-53.

Boulin, T., J. F. Etchberger, et al. (2006). "Reporter gene fusions." WormBook: 1-23.

Ceron, J., J. F. Rual, et al. (2007). "Large-scale RNAi screens identify novel genes that interact with the C. elegans retinoblastoma pathway as well as splicing-related components with synMuv B activity." BMC Dev Biol **7**: 30.

Chalfie, M., Y. Tu, et al. (1994). "Green fluorescent protein as a marker for gene expression." Science **263**(5148): 802-5.

Chokroverty, S., W. Nicklas, et al. (1990). "Multiple system degeneration with glutamate dehydrogenase deficiency: pathology and biochemistry." J Neurol Neurosurg Psychiatry **53**(12): 1099-101.

Clark, D. V., T. M. Rogalski, et al. (1988). "The unc-22(IV) region of Caenorhabditis elegans: genetic analysis of lethal mutations." Genetics **119**(2): 345-53.

Clark, D. V. (1990). The *unc-22 IV* region of *Caenorhabditis elegans*: genetic analysis and molecular mapping. Burnaby, B.C., Simon Fraser University. **Ph.D. Thesis**.

Clark, D. V. and D. L. Baillie (1992). "Genetic analysis and complementation by germ-line transformation of lethal mutations in the unc-22 IV region of Caenorhabditis elegans." Mol Gen Genet **232**(1): 97-105.

Dieter, H., R. Koberstein, et al. (1981). "Studies of glutamate dehydrogenase. The interaction of ADP, GTP, and NADPH in complexes with glutamate dehydrogenase." Eur J Biochem **115**(1): 217-26.

Elion, E. A., B. Satterberg, et al. (1993). "FUS3 phosphorylates multiple components of the mating signal transduction cascade: evidence for STE12 and FAR1." Mol Biol Cell **4**(5): 495-510.

Fernandez, A. G., K. C. Gunsalus, et al. (2005). "New genes with roles in the C. elegans embryo revealed using RNAi of ovary-enriched ORFeome clones." Genome Res **15**(2): 250-9.

Fire, A., S. Xu, et al. (1998). "Potent and specific genetic interference by double-stranded RNA in Caenorhabditis elegans." Nature **391**(6669): 806-11.

Frigerio, F., M. Casimir, et al. (2008). "Tissue specificity of mitochondrial glutamate pathways and the control of metabolic homeostasis." Biochim Biophys Acta **1777**(7-8): 965-72.

Herman, R. K. (1984). "Analysis of genetic mosaics of the nematode Caneorhabditis elegans." Genetics **108**(1): 165-80.

Hirsh, D., D. Oppenheim, et al. (1976). "Development of the reproductive system of Caenorhabditis elegans." Dev Biol **49**(1): 200-19.

Hobert, O. (2002). "PCR fusion-based approach to create reporter gene constructs for expression analysis in transgenic C. elegans." Biotechniques **32**(4): 728-30.

Kamath, R. S., A. G. Fraser, et al. (2003). "Systematic functional analysis of the Caenorhabditis elegans genome using RNAi." Nature **421**(6920): 231-7.

Kao, G., C. Nordenson, et al. (2007). "ASNA-1 positively regulates insulin secretion in C. elegans and mammalian cells." Cell **128**(3): 577-87.

Kimble, J. and D. Hirsh (1979). "The postembryonic cell lineages of the hermaphrodite and male gonads in Caenorhabditis elegans." Dev Biol **70**(2): 396-417.

Lall, S., D. Grun, et al. (2006). "A genome-wide map of conserved microRNA targets in C. elegans." Curr Biol **16**(5): 460-71.

Li, W., S. G. Kennedy, et al. (2003). "daf-28 encodes a C. elegans insulin superfamily member that is regulated by environmental cues and acts in the DAF-2 signaling pathway." Genes Dev **17**(7): 844-58.

Lim, L. P., N. C. Lau, et al. (2003). "The microRNAs of Caenorhabditis elegans." Genes Dev **17**(8): 991-1008.

Liu, H., C. A. Styles, et al. (1993). "Elements of the yeast pheromone response pathway required for filamentous growth of diploids." Science **262**(5140): 1741-4.

Livak, K. J. and T. D. Schmittgen (2001). "Analysis of relative gene expression data using real-time quantitative PCR and the 2(-Delta Delta C(T)) Method." Methods **25**(4): 402-8.

Marra, M. A. (1994). Genome analysis in *C. elegans*: genetic and molecular identification of genes tightly linked to *unc-22(IV)*. Burnaby, B.C., Simon Fraser University. **Ph.D. Thesis**.

Marra, M. A., S. S. Prasad, et al. (1993). "Molecular analysis of two genes between let-653 and let-56 in the unc-22(IV) region of Caenorhabditis elegans." Mol Gen Genet **236**(2-3): 289-98.

Martin, G., K. Schouest, et al. (2007). "Prediction and validation of microRNA targets in animal genomes." J Biosci **32**(6): 1049-52.

McKay, S. J., R. Johnsen, et al. (2003). "Gene expression profiling of cells, tissues, and developmental stages of the nematode C. elegans." Cold Spring Harb Symp Quant Biol **68**: 159-69.

Moerman, D. G. and D. L. Baillie (1979). "Genetic Organization in CAENORHABDITIS ELEGANS: Fine-Structure Analysis of the unc-22 Gene." Genetics **91**(1): 95-103.

Ogg, S., S. Paradis, et al. (1997). "The Fork head transcription factor DAF-16 transduces insulin-like metabolic and longevity signals in C. elegans." Nature **389**(6654): 994-9.

Prasad, S. S. and D. L. Baillie (1989). "Evolutionarily conserved coding sequences in the dpy-20-unc-22 region of Caenorhabditis elegans." Genomics **5**(2): 185-98.

Rogalski, T. M. and D. L. Baillie (1985). "Genetic organization of the unc-22 IV gene and the adjacent region in Caenorhabditis elegans." Mol Gen Genet **201**(3): 409-14.

Rogalski, T. M., D. G. Moerman, et al. (1982). "Essential genes and deficiencies in the unc-22 IV region of Caenorhabditis elegans." Genetics **102**(4): 725-36.

Rual, J. F., J. Ceron, et al. (2004). "Toward improving Caenorhabditis elegans phenome mapping with an ORFeome-based RNAi library." Genome Res **14**(10B): 2162-8.

Schmittgen, T. D. and K. J. Livak (2008). "Analyzing real-time PCR data by the comparative C(T) method." Nat Protoc **3**(6): 1101-8.

Sener, A. and W. J. Malaisse (1980). "L-leucine and a nonmetabolized analogue activate pancreatic islet glutamate dehydrogenase." Nature **288**(5787): 187-9.

Smith, T. J. and C. A. Stanley (2008). "Untangling the glutamate dehydrogenase allosteric nightmare." Trends Biochem Sci **33**(11): 557-64.

Solomon, S. S., G. Majumdar, et al. (2008). "A critical role of Sp1 transcription factor in regulating gene expression in response to insulin and other hormones." Life Sci **83**(9-10): 305-12.

Sonnichsen, B., L. B. Koski, et al. (2005). "Full-genome RNAi profiling of early embryogenesis in Caenorhabditis elegans." Nature **434**(7032): 462-9.

Stanley, C. A., Y. K. Lieu, et al. (1998). "Hyperinsulinism and hyperammonemia in infants with regulatory mutations of the glutamate dehydrogenase gene." N Engl J Med **338**(19): 1352-7.

Sulston, J. E., E. Schierenberg, et al. (1983). "The embryonic cell lineage of the nematode Caenorhabditis elegans." Dev Biol **100**(1): 64-119.

Yamamoto, M., S. Takahashi, et al. (1997). "Upstream and downstream of erythroid transcription factor GATA-1." Genes Cells **2**(2): 107-15.

Zhu, J., R. J. Hill, et al. (1997). "end-1 encodes an apparent GATA factor that specifies the endoderm precursor in Caenorhabditis elegans embryos." Genes Dev **11**(21): 2883-96.